
DENSITY REGRESSION WITH BAYESIAN ADDITIVE REGRESSION TREES

A PREPRINT

Vittorio Orlandi
Dept. of Statistical Science
Duke University
Durham, NC 27708
vdo@duke.edu

Jared Murray
Dept. of Information,
Risk, and Operations Management
University of Texas, Austin
Austin, TX 78712
jared.murray@mcombs.utexas.edu

Antonio Linero
Dept. of Statistics and Data Sciences
University of Texas, Austin
Austin, TX 78712
antonio.linero@austin.utexas.edu

Alexander Volfovsky
Dept. of Statistical Science
Duke University
Durham, NC 27708
alexander.volfovsky@duke.edu

December 24, 2021

ABSTRACT

Flexibly modeling how an entire density changes with covariates is an important but challenging generalization of mean and quantile regression. While existing methods for density regression primarily consist of covariate-dependent discrete mixture models, we consider a continuous latent variable model in general covariate spaces, which we call DR-BART. The prior mapping the latent variable to the observed data is constructed via a novel application of Bayesian Additive Regression Trees (BART). We prove that the posterior induced by our model concentrates quickly around true generative functions that are sufficiently smooth. We also analyze the performance of DR-BART on a set of challenging simulated examples, where it outperforms various other methods for Bayesian density regression. Lastly, we apply DR-BART to two real datasets from educational testing and economics, to study student growth and predict returns to education. Our proposed sampler is efficient and allows one to take advantage of BART's flexibility in many applied settings where the entire distribution of the response is of primary interest. Furthermore, our scheme for splitting on latent variables within BART facilitates its future application to other classes of models that can be described via latent variables, such as those involving hierarchical or time series data.

Keywords Bayesian Nonparametrics · Conditional Density Estimation · Posterior Concentration · Latent Variables · Heteroscedasticity

1 Introduction

Data analysis frequently concerns itself with associating the change in a function of some response variable y with a set of covariates \mathbf{x} . Arguably the most common tool for this is mean regression, which focuses on the expectation $E[y | \mathbf{x}]$ and foregoes inference about other parts of the conditional density $p(y | \mathbf{x})$, a much more general quantity. This inflexibility has been recognized as problematic in many modern applications [see, e.g. Wittman, 2009, Karabatsos and Walker, 2011, Gneiting and Katzfuss, 2014]. It is then natural to ask if other functionals of $p(y | \mathbf{x})$ are more appropriate, with two immediate candidates: quantile regression and density regression.

Quantile regression models specific quantiles of the conditional response distribution. This can help address settings where some quantiles carry more probative value. For example, Black et al. [2007] note that the impact of a job training

program on the upper quantiles of the distribution is considered to be more important by policy makers than that on the lower quantiles. While this approach is more general than mean regression, one problem with its application is that computing estimates of functionals of the quantiles is not always straightforward. Another problem is that estimated quantiles oftentimes do not obey the monotonicity constraint inherently satisfied by the true distribution. While there are approaches for joint modeling of quantiles (e.g. Kadane and Tokdar [2012], Sangnier et al. [2016]) or post-hoc reordering of estimates (e.g. Chernozhukov et al. [2010]), the fundamental limitation with the approach is that individual quantiles are being targeted as proxies for features of the distribution as a whole.

By modeling the entire probability distribution of the response, density regression methods perform a substantially harder task than mean or even quantile regression. In doing so, however, they are able to compute coherent point estimates and perform uncertainty quantification for arbitrary functionals of the distribution that may be of interest. Studies of income inequality, for example, typically take into account the impact of variables on the entire income distribution [e.g. Gerfin, 1994, Daly and Valletta, 2006]. To date, there is a large literature on density regression. We contribute to this body of work by providing a general, yet reasonably structured, formulation of the problem that enjoys important theoretical guarantees and yields an efficient sampler with strong empirical performance.

In this work, we consider the following model for the conditional density:

$$p(y | \mathbf{x}, f, \sigma) = \int_0^1 \frac{1}{\sigma(\mathbf{x}, u)} \phi\left(\frac{y - f(\mathbf{x}, u)}{\sigma(\mathbf{x}, u)}\right) du, \quad (1)$$

which is parameterized by the latent variable u . This model generalizes the covariate dependent mixture model discussed in detail below. At the same time, it posits a fairly specific form by which f and σ interact to generate a conditional density. Various forms of this model have been considered in Pati et al. [2011], Kundu and Dunson [2014], and Zhou et al. [2017], where Gaussian process priors were placed on $f(x, u)$ and inverse gamma priors on either $\sigma(x, u) = \sigma$ or $\sigma^2(x, u) = \sigma^2$. Instead, we propose placing BART-type priors on both f and σ . While BART was designed for mean regression, we also consider a modification allowing it to model variance function to grant the model added flexibility in finite sample settings, and generalize both to accommodate latent variables. Asymptotically, we show that the posterior specified by our model concentrates around a true underlying density, provided its log is α -Hölder for $0 < \alpha \leq 2$. The rate of concentration is removed from the minimax rate by a factor of $\alpha/(\alpha + 1)$ because BART generates piecewise constant functions; however, a near-minimax rate can be attained by using the SBART model of Linero and Yang [2018] and restricting to a slightly smaller function class. In addition to yielding a more efficient sampler, we also show that this model outperforms its counterpart employing Gaussian process priors, as well as a variety of other methods for density regression in several empirical evaluations.

We also apply our method to two real world datasets. In the first, we compute quantile growth targets for students in elementary and middle school mathematics classes using data provided in Betebenner et al. [2011]. Mean regression approaches fail to identify interesting aspects of the data — such as that conditional distributions of test scores become more skewed over time — and quantile regression approaches can suffer from quantile crossing and a limited description of the uncertainty in their estimates. Our model addresses both these problems simultaneously. In the second, we study returns to education from US census microdata originally compiled by Angrist et al. [2006]. The returns are a nonlinear functional of quantiles of the wage distribution and therefore well suited for analysis by density regression methods, which fully capture uncertainty about their estimates.

The paper proceeds as follows. The remainder of the introduction discusses past work on density regression models. Section 2 gives a brief overview of BART and its application to modeling mean and variance functions. In Section 3, we motivate our use of BART for modeling components of the conditional density and state our full model for density regression, which we refer to as DR-BART. Section 4 outlines theoretical results concerning our model, namely the rate at which the posterior contracts about a true density. Section 5 compares DR-BART to other models for density regression on a variety of simulated datasets and Section 6 applies DR-BART to two real world datasets from education and economics. Section 7 concludes.

1.1 Related Work

Our proposal generalizes a common approach to density regression that uses covariate dependent mixture models. In these models, the conditional density is given by:

$$p(y | \mathbf{x}, \theta, \pi) = \sum_{h=1}^k \pi_h(\mathbf{x}) \mathcal{K}(y; \theta_h(\mathbf{x})), \quad (2)$$

allowing for $k = \infty$, where $\mathcal{K}(\cdot, \cdot)$ is a positive definite kernel function and $\pi_h(\mathbf{x})$ are covariate-dependent mixture weights. We restrict attention to normal kernels:

$$p(y | \mathbf{x}, \theta \equiv (\mu, \sigma), \pi) = \sum_{h=1}^k \pi_h(\mathbf{x}) \phi_{\sigma_h(\mathbf{x})}(y - \mu_h(\mathbf{x})), \quad (3)$$

where $\phi_\sigma(z) = (1/\sigma)\phi(z/\sigma)$ and ϕ denotes the standard normal pdf – but the extension to other kernels is straightforward. In practice π or θ may not vary with \mathbf{x} , or may vary in a limited way. (e.g., by taking $\mu_h(\mathbf{x}) = \mathbf{x}'\beta_h$, $\sigma_h(\mathbf{x}) = \sigma_h$). Our proposed model in (1) recovers that in (3) when f and σ are step functions with the same points of discontinuity (which can depend on the covariates).

Models of the form in (3) appear in the machine learning literature as “mixtures of experts” [Jacobs et al., 1991, Jordan and Jacobs, 1994] where the initial focus was on using these models for flexible mean regression or classification. Geweke and Keane [2007] and Villani et al. [2009] study models of this form for semiparametric density regression, using finite k and multinomial probit and logit regression models for $\pi(\mathbf{x})$. While it is possible to get consistency properties for large classes of conditional densities (see e.g. Norets et al. [2010], Pati et al. [2013], Norets and Pelenis [2014] and the monograph Norets and Pati [2014]), practical experience in finite samples suggests that there can be value in allowing the kernel variance to depend on \mathbf{x} , as this can reduce the number of clusters required for an accurate approximation. Villani et al. [2009] provide simulated examples and discussion in the case of fixed k , and we will revisit this point in the context of the models introduced here (Section 5).

Another approach proposes to leverage the joint model for (y, \mathbf{x}) as a convenient device for inducing a particular conditional model as $p(y | \mathbf{x}, \theta) = p(y, \mathbf{x} | \theta)/p(\mathbf{x} | \theta)$ (as in e.g. Muller et al. [1996], Park and Dunson [2010], among others). There is some cost to the joint modeling approach – which itself has commanded a large literature (see West and Escobar [1993], Muller et al. [1996] and variations in Shahbaba and Neal [2009], Taddy and Kottas [2010], Molitor et al. [2010], Wade et al. [2011], Dunson and Bhattacharya [2011], Hannah et al. [2011], Wade et al. [2014]) – in terms of computation and accuracy as the dimension of the covariate vector grows (see Hannah et al. [2011], Wade et al. [2014]). The posterior can also depend on the distribution of the covariates, even when care is taken to separate the parameter spaces in the prior, as the auxiliary joint model assumes a common clustering for the response and the covariates (see Griffin’s discussion of Dunson and Bhattacharya [2011]; also, Walker and Karabatsos [2013] and Wade et al. [2014]). Thus, other nonparametric Bayesian models focus explicitly on the conditional distributions of interest; these date to (at least) MacEachern’s seminal work on dependent Dirichlet processes (DDPs) [MacEachern, 1999, 2000]. A DDP is a prior for a collection of distributions such that at each covariate value the process is marginally a DP. Models in this class include De Iorio et al. [2004], Griffin and Steel [2006], Dunson and Peddada [2008], De Iorio et al. [2009], Wang and Dunson [2011], and numerous other specializations to spatiotemporal or hierarchical models. Barrientos et al. [2012] characterize the DDP in terms of copulas and provide results about its support and about kernel mixtures using the DDP.

2 Heteroscedastic Regression with BART priors

2.1 Bayesian Additive Regression Trees (BART)

Bayesian Additive Regression Trees (BART) were introduced by Chipman et al. [2010] (henceforth CGM) as a nonparametric prior over a regression function f designed to capture complex, nonlinear relationships and interactions. Specifically, for observed data pairs $\mathcal{D} = \{(y_i, \mathbf{x}_i); 1 \leq i \leq n\}$, CGM propose the regression model:

$$y_i = f(\mathbf{x}_i) + \epsilon_i, \quad \epsilon_i \stackrel{iid}{\sim} N(0, \sigma^2). \quad (4)$$

The BART prior represents f as the sum of many piecewise constant regression trees. Each tree T_h , $1 \leq h \leq m$ consists of a set of interior decision nodes (where decisions are generally of the form $x_j < c$ for some value c) and a set of b_h terminal nodes. The terminal nodes have associated parameters $M_h = (\mu_{h1}, \mu_{h2}, \dots, \mu_{hb_h})'$. For each tree there is a partition of the covariate space $\{\mathcal{A}_{h1}, \dots, \mathcal{A}_{hb_h}\}$ with each element of the partition corresponding to a terminal node. A tree and its associated parameters define step functions:

$$g(\mathbf{x}, T_h, M_h) = \mu_{hb} \text{ if } \mathbf{x} \in \mathcal{A}_{hb} \text{ (for } 1 \leq b \leq b_h). \quad (5)$$

These functions are additively combined to obtain f :

$$f(\mathbf{x}) = \sum_{h=1}^m g(\mathbf{x}, T_h, M_h). \quad (6)$$

This model has been shown empirically and theoretically (see, e.g. Chipman et al. [2010], Jeong and Rockova [2020]) to be accurate, highly flexible, and robust to the presence of irrelevant covariates. The default prior parameters work very well in practice and the model admits an efficient sampler. More details on BART can be found in the Supplement.

2.2 A BART prior for variance functions

As mentioned in the introduction, to allow for flexible density regression in finite samples, it may be useful to allow the variance of the process to depend on \mathbf{x} as well. To this end, we adopt the log-linear BART prior of Murray [2021] for the log-variance. Specifically, consider the heteroskedastic regression problem $y_i = f(\mathbf{x}) + \sigma^2(\mathbf{x})\epsilon_i$ where $\epsilon_i \stackrel{iid}{\sim} N(0, \sigma_0^2)$. Murray places a log-linear BART prior on $\sigma^2(\cdot)$:

$$\log[\sigma^2(\mathbf{x})] = \sum_{h=1}^{m_v} g(\mathbf{x}, T_h^{(v)}, M_h^{(v)}),$$

where $\{(T_h^{(v)}, M_h^{(v)})\}$ are trees and parameters for the variance function. The prior for the exponentiated leaf parameters $\exp(\mu_{hb}^{(v)})$ is conjugate, symmetric on the log scale, and can be calibrated to match the expected prior range of the log-variance process. More details on BART's extension to log-linear models can be found in the Supplement.

3 Density Regression with BART priors

Even with a flexible variance function, the normality assumption of heteroscedastic BART may be too restrictive; for example, at any covariate value it yields symmetric predictive distributions. In this section, we extend the heteroscedastic BART model to general density regression problems by introducing a continuous latent variable U , which is treated as an omitted variable independent of \mathbf{x} . Before introducing the model in full generality we will motivate the use of continuous latent variables in the density estimation setting.

3.1 Continuous latent variable priors for a single density

Consider the following generalized location model for estimating a single density:

$$p(y) = \int_0^1 \phi_\sigma(y - f(u)) du. \quad (7)$$

An equivalent representation in terms of a latent variable is

$$Y = f(U) + \epsilon, \quad U \sim U(0, 1), \quad \epsilon \sim N(0, \sigma^2) \quad (8)$$

where (7) is obtained on marginalizing over U . In the limit as $\sigma \rightarrow 0$, $Y \stackrel{d}{=} f(U)$ where $U \sim U(0, 1)$. This class of models can be quite broad, depending on the prior for f ; if f is the quantile function of a distribution P , then $Y \sim P$. We do not restrict f to be monotone; while it would be possible to do so, this substantially increases the computational burden and since subsequent inference is on the induced density for y (or $y \mid \mathbf{x}$ below) or its functionals rather than f itself, the monotonicity constraint is not necessary.

Discrete location mixtures arise as a special case of this model when f is a step function. Suppose $f(u) = \mu_h$ for $u \in [\nu_h, \nu_{h+1})$, where ν is an increasing sequence on $[0, 1)$ such that $\nu_1 = 0$ and $\sum_{h=0}^{\infty} (\nu_{h+1} - \nu_h) = 1$. Then we have:

$$p(y) = \int_0^1 \phi_\sigma(y - \mu_h) \mathbf{1}(u \in [\nu_h, \nu_{h+1})) du = \sum_{h=1}^{\infty} (\nu_{h+1} - \nu_h) \phi_\sigma(y - \mu_h).$$

This representation is intimately related to the augmented model used for slice sampling infinite mixture models [Walker, 2007, Kalli et al., 2011], where a prior on f is induced via the prior on mixture component weights $\pi_h \equiv \nu_{h+1} - \nu_h$.

Priors on mixture weights are only one way to induce the prior on f . Kundu and Dunson [2014] proposed placing a Gaussian process prior directly on f , suggesting models centered on a prior guess of the quantile function and using a squared exponential covariance function. Theoretically, this is a flexible choice [see Pati et al., 2011, Kundu and Dunson, 2014]; however, it introduces computational difficulties, requiring a discretization of the space that may reduce the quality of the subsequent inference. Furthermore, it is not immediately clear how to introduce multiple or categorical covariates into this framework.

The continuous latent variable model is appealing, however. In many contexts it is more intuitive to think of distributional features as arising from some omitted or latent continuous variables, and not from heterogeneity due to multiple independent subpopulations. Adapting BART to this setting yields priors for f which incorporate covariates flexibly, are approximately smooth, and do not require discretization of the latent variable *a priori*.

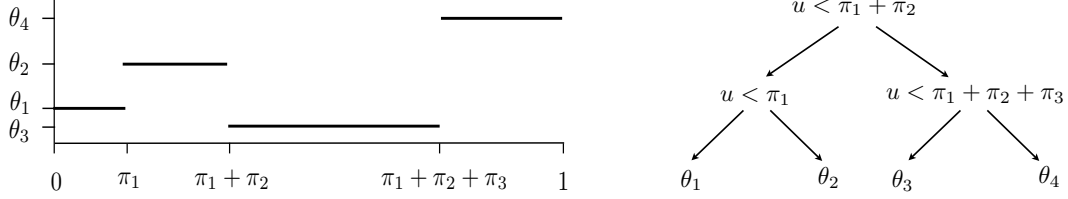


Figure 1: Representing a step function (left) as a binary tree (right).

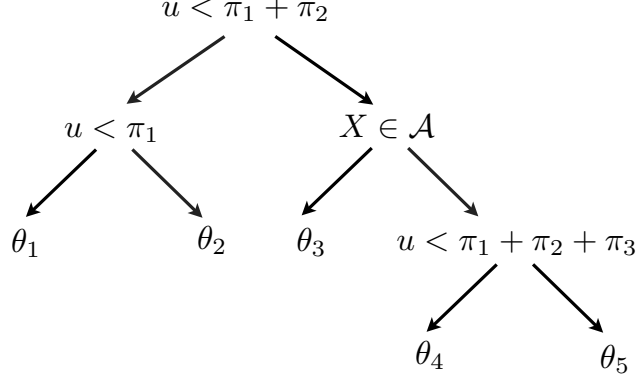


Figure 2: Modifying the tree in Fig. 1 to incorporate covariates

3.2 Density Regression with BART (DR-BART)

To motivate the use of tree-based priors, recall that the normal location mixture model corresponds to a step function for f , which can also be represented as a binary tree (Fig. 1). In the tree-based representation, incorporating covariates is simply a matter of introducing additional covariate-based splitting rules; Figure 2 modifies the tree to split on \mathbf{x} . Marginalizing over the latent variable in this example gives the two conditional densities:

$$p(y | \mathbf{x} \in A) = \pi_1 \phi_\sigma(y - \theta_1) + \pi_2 \phi_\sigma(y - \theta_2) + (\pi_3 + \pi_4) \phi_\sigma(y - \theta_3) \quad (9)$$

$$p(y | \mathbf{x} \notin A) = \pi_1 \phi_\sigma(y - \theta_1) + \pi_2 \phi_\sigma(y - \theta_2) + \pi_3 \phi_\sigma(y - \theta_4) + \pi_4 \phi_\sigma(y - \theta_5) \quad (10)$$

The resulting model has some interesting properties. There are shared components and shared weights (e.g. θ_1, θ_2 and π_1, π_2) but also components and weights that are unique to each conditional distribution (e.g. $\pi_3 + \pi_4$ versus π_3, π_4). This allows borrowing of information across the covariate space, with the degree of borrowing controlled by the tree structure. Trees with multiple interior splits on \mathbf{x} allow the model to capture multiscale structure, as the degree of borrowing varies across the covariate space. In the extreme case, a tree that splits on \mathbf{x} before splitting on U will yield two independent density estimates, while a tree that doesn't split on U yields a standard Bayesian CART model.

In practice, a single tree model will probably be inadequate for many applications. With many covariates, nearly smooth mean functions, or highly skewed/multimodal distributions the tree will have to grow quite large. Additionally, the presence of the latent variable U will tend to yield poor mixing and further complicate the design of MCMC algorithms for the single tree model (see Chipman et al. [1998], Denison et al. [1998] for discussion of the complications arising in MCMC for single tree models *without* latent variables).

A BART prior for f is a natural alternative to a single tree model and additional flexibility can be obtained by modeling the variance function as well. For density regression we modify both BART priors from Section 2 to include a latent variable U . The most general model for density regression with BART (DR-BART) is:

$$U \sim U[0, 1], \quad \epsilon \sim N(0, \sigma_0^2) \quad (11)$$

$$Y = f(\mathbf{x}, U) + \exp[v(\mathbf{x}, U)/2]\epsilon. \quad (12)$$

Letting $\sigma(\mathbf{x}, u) = \exp[v(\mathbf{x}, u)/2]\sigma_0$, the density function at \mathbf{x} is

$$p(y | \mathbf{x}) = \int_0^1 \phi_{\sigma(\mathbf{x}, u)}(y - f(\mathbf{x}, u)) du, \quad (13)$$

a location-scale mixture of normals. In addition to the full DR-BART model, two reduced models are potentially of interest:

1. Location-only mixture (DR-BART-L): Constant bandwidth, $\sigma(\mathbf{x}, u) \equiv \sigma_0$
2. Location mixture with heteroscedasticity (DR-BART-LH): Covariate-dependent bandwidth parameter, $\sigma(\mathbf{x}, u) \equiv \sigma(\mathbf{x}) = \exp[v(\mathbf{x})/2]\sigma_0$

Priors for the DR-BART parameters are specified as follows:

- f , the location function: The CGM BART prior with $k = 2$ and $m = 250$ trees. We also require that the leaves of each tree contain at least 5 observations. In the context of DR-BART this condition is related to priors on mixture models for a single density that require all the components to be occupied (see e.g. Diebolt and Robert [1994]).
- v , the bandwidth function: The BART variance prior from Section 2, with 100 trees and a_0 (a hyperparameter for $\sigma(\mathbf{x}, u)$ defined in the Supplement) calibrated to a reasonable range, as described in the Supplement.
- Depending on the model, σ_0^2 is either fixed (DR-BART, DR-BART-LH) or given a further inverse gamma prior (DR-BART-L): $\sigma_0^2 \sim IG(\nu_0/2, \nu_0\xi_0/2)$, with ξ_0 a prior guess at an appropriate bandwidth. In DR-BART-L, posterior inferences are insensitive to reasonable specifications of ξ_0 , but allowing $\nu_0 \rightarrow 0$ puts too much mass near 0. Since σ_0^2 is not identified separately from the flexible variance function ν in the full DR-BART/DR-BART-LH models, the prior should be very informative and in practice fixing it at a sensible guess (some fraction of the sample variance or of the variance of the OLS residuals) seems to work well. It could also be elicited more formally.

Results appear to be more or less insensitive to the numbers of trees in f and v provided they are large enough, and the values chosen here reflect experience with mean regression BART and the belief that variance functions are less complex than location functions.

Before describing posterior sampling we will describe the properties of f and v and provide some intuition for their roles in the model.

3.2.1 The location function f

With a BART prior for f , $f(\mathbf{x}, u)$ decomposes as

$$f(\mathbf{x}, u) = \sum_{h=1}^m g(\mathbf{x}, u, T_h, M_h) \equiv f_x(\mathbf{x}) + f_{xu}(\mathbf{x}, u) + f_u(u). \quad (14)$$

The three functions in (14) are defined (from left to right) as the sum of the trees splitting only on \mathbf{x} , on both \mathbf{x} and u , and only on u . These terms can capture covariate effects that are pure location shifts, covariate-dependent distributional features, and distributional features common across covariate space (respectively). Using posterior samples of the trees to try to infer which variables influence the responses and in what manner is somewhat fraught, however. For example, it is possible that a tree in $f_{xu}(\mathbf{x}, u)$ split trivially on U in that the leaf parameters on either side of the split are nearly identical or cancelled by the contribution of other trees. This is essentially the same difficulty reported by CGM in doing variables selection in BART mean regression by counting the trees splitting on a particular variable. But (14) does give some insight into how the model *can* capture the complex effects that \mathbf{x} may have on the distribution of Y , even with a constant bandwidth.

Since f and v are step functions, this model is equivalent to a discrete mixture of normal distributions. But the prior is much different than the usual priors in covariate-dependent mixture models. First, the number of distinct mixture components with positive probability varies across covariate space like in the single tree model. Second, unlike in the single tree model, the components are correlated *a priori*; given a fixed set of m trees T we have:

$$\text{Cov}(f(\mathbf{x}, u), f(\mathbf{x}', u')) = \sigma_\mu^2 \mathcal{N}[(\mathbf{x}, u), (\mathbf{x}', u')] \quad (15)$$

$$\text{Cor}(f(\mathbf{x}, u), f(\mathbf{x}', u')) = \mathcal{N}[(\mathbf{x}, u), (\mathbf{x}', u')]/m \quad (16)$$

where $\mathcal{N}[(\mathbf{x}, u), (\mathbf{x}', u')]$ is the number of trees where (\mathbf{x}, u) and (\mathbf{x}', u') are in the same leaf. It follows from (16) that if $|u - u'| > |u - u''|$, then

$$\text{Cov}(f(\mathbf{x}, u), f(\mathbf{x}, u')) \geq \text{Cov}(f(\mathbf{x}, u), f(\mathbf{x}, u'')) \quad (17)$$

$$\text{Cor}(f(\mathbf{x}, u), f(\mathbf{x}, u')) \geq \text{Cor}(f(\mathbf{x}, u), f(\mathbf{x}, u'')). \quad (18)$$

Given the potentially strong correlation, it is misleading to think of the steps in f as ‘‘mixture components’’ in the usual sense.

3.2.2 The bandwidth function v

A covariate-adaptive bandwidth parameter will often be important in these models. Since U and ϵ are independent, in the DR-BART-L model $\text{Var}(Y | \mathbf{x}) \geq \text{Var}(\sigma_0 \epsilon) = \sigma_0^2$. On the other hand, in the DR-BART-LH model $\text{Var}(Y | \mathbf{x}) \geq \text{Var}(\exp[v(\mathbf{x})/2]\epsilon) = \sigma(\mathbf{x})^2$. In a model without a covariate adaptive bandwidth, σ_0^2 must be at least as small as the most concentrated predictive density to avoid oversmoothing, yielding much rougher density estimates elsewhere. The efficiency of the MCMC sampler suffers as well, as smaller bandwidths imply more concentrated distributions for U_i . A covariate dependent bandwidth might be preferable for this reason, even if a single bandwidth seems like a reasonable simplification.

The full DR-BART model has an additional degree of flexibility due to scale mixing. It can allow $v(\mathbf{x}, u)$ to grow large in some areas of U -space, effectively “turning off” portions of $f(\mathbf{x}, u)$ or capturing relatively flat areas of the density. The behavior of the different models is easiest to understand with an example, presented in Section 5.

3.2.3 Posterior Sampling

Generating samples from the posterior with MCMC is straightforward. Conditional on values for the latent variables $u = (u_1, u_2, \dots, u_n)$, DR-BART reduces to the heteroscedastic BART model so that sampling for the other parameters proceeds as described in the Supplement. The latent u_i have full conditionals

$$p(u_i | -) \propto \phi_{\sigma(\mathbf{x}, u)}(y - f(\mathbf{x}, u)) \mathbf{1}(u \in \mathcal{B}(T, T^{(v)})), \quad (19)$$

where $\mathcal{B}(T, T^{(v)})$ is the set of possible u -values; that is, those that do not yield trees with leaves having fewer than 5 observations. Since f and σ are step functions, (19) is piecewise constant, so u_i can be updated with a Gibbs step: If $u_1^* < u_2^* < \dots < u_k^*$ are the points of discontinuity of (19) and $u_0^* = 0$, $u_{k-1}^* = 1$, the Gibbs step first samples an interval from

$$\Pr(u_i \in (u_h^*, u_{h+1}^*) | -) \propto \phi_{\sigma(\mathbf{x}, \tilde{u}_h)}(y - f(\mathbf{x}, \tilde{u}_h)) \mathbf{1}(u \in \mathcal{B}(T, T^{(v)})), \quad (20)$$

where $\tilde{u}_h = (u_{h+1}^* - u_h^*)/2$ (or any other point in the interval) and then u_i is sampled uniformly from the selected interval. Note that $\mathbf{1}(u \in \mathcal{B}(T, T^{(v)}))$ necessarily equals either 0 or 1 on the entire interval (u_h^*, u_{h+1}^*) for each h by construction.

While conceptually simple, the Gibbs sampling update can require a large number of likelihood evaluations (k is often well into the hundreds). On the other hand, a Metropolis step is difficult to tune because (19) is in general multimodal. An efficient alternative that doesn’t require tuning is slice sampling which introduces latent variables ω_i so that

$$p(\omega_i, u_i | -) \propto \mathbf{1}(\omega_i < \phi_{\sigma(\mathbf{x}, u)}(y - f(\mathbf{x}, u))) \mathbf{1}(u \in \mathcal{B}(T, T^{(v)})). \quad (21)$$

Sampling proceeds using the techniques developed in Neal [2003]. The slice sampler is much more efficient, which tends to make up for any loss in theoretical efficiency or mixing.

4 Theory

Here, we present some properties of the DR-BART model, showing that our proposed prior generates trees that are almost surely finite and upper bounding the rate at which DR-BART estimates the conditional density $p(y | \mathbf{x})$. We focus on the special case where the predictors $\mathbf{x}_i \in [0, 1]^p$ are continuous. This is a common assumption when studying theoretical properties of density regression models [e.g. Chung and Dunson, 2012, Pati et al., 2013, Li et al., 2020]. The assumption is even more innocuous here, as BART is invariant to monotone transformations of the covariates. Proofs can be found in the Supplement.

Theorem 1. *Assume that the prior over a binary tree is as in CGM, but with a continuous uniform prior on splitting locations and no restriction to nonempty leaves. A tree sampled from this prior has finite depth with probability one.*

Thus, introducing a latent u into the prior does not affect the finite depth of the trees. We now focus on providing upper bounds for the posterior concentration rate ϵ_n of the posterior. A rate $\epsilon_n \downarrow 0$ is said to be a *rate of convergence* of the posterior with respect to a divergence measure h if there exists a positive constant M such that $\Pi\{h(p_0, p_{f, \sigma}) \geq M \epsilon_n | \mathcal{D}_n\} \rightarrow 0$ in F_0 -probability, where $\mathcal{D}_n = \{(\mathbf{X}_i, Y_i) : i = 1 \dots, n\}$ and $(\mathbf{X}_i, Y_i) \stackrel{iid}{\sim} F_0(d\mathbf{x}, dy) = p_0(y | \mathbf{x}) dy F_{\mathbf{X}}(d\mathbf{x})$.

The conditional density of y induced by our model is given by the convolution

$$p_{f, \sigma}(y | \mathbf{x}) = \int \phi_{\sigma(\mathbf{x}, u)}(y - f(\mathbf{x}, u)) du,$$

and the limit $\sigma(\mathbf{x}, u) \rightarrow 0$ is associated with a random variable with quantile function $f(\mathbf{x}, u)$ if $f(\mathbf{x}, u)$ is monotonically increasing in u . This suggests that a reasonable strategy for establishing that $p_{f,\sigma}$ is close to p_0 is to show that $f(\mathbf{x}, u)$ is close to the true conditional quantile function $f_0(\mathbf{x}, u)$.

We characterize the concentration of DR-BART with respect to the integrated Hellinger distance, defined: $h(p, q) = \left(\int (\sqrt{p(y|\mathbf{x})} - \sqrt{q(y|\mathbf{x})})^2 dy F_{\mathbf{X}}(d\mathbf{x}) \right)^{1/2}$. Two other divergence measures which will be useful for us are the *generalized Kullback-Leibler divergences* $\text{KL}(p_1 \| p_2) = \int p_1 \log(p_1/p_2) dy F_{\mathbf{X}}(d\mathbf{x})$ and $V(p_1 \| p_2) = \int p_1 \log^2(p_1/p_2) dy F_{\mathbf{X}}(d\mathbf{x})$.

To study the posterior concentration of DR-BART, we make use of results from (i) Jeong and Rockova [2020] involving the concentration of BART in a regression setting and (ii) Pati et al. [2011], Zhou et al. [2017] who leverage similar results about Gaussian processes to show convergence in a latent variable model similar to the one considered here. Our proof extends both of these works in fundamental ways. We extend Jeong and Rockova [2020] by introducing latent variables into the tree structure. While having immediate implications for DR-BART this also lays the groundwork for concentration results for latent variable BART models that we will consider in the future. Compared to Pati et al. [2011], we not only introduce covariates into the setup, but also place a non-trivial DR-BART prior over the bandwidth, compared to their choice of a parametric, covariate-independent prior.

Next, we outline conditions required for our proof. Throughout, we will write $a \lesssim b$ to mean that there exists a positive constant C , possibly depending on p_0 and on hyperparameters but otherwise independent of n, p , or any other variables, such that $a \leq Cb$.

Condition F (on p_0) We assume that $\log p_0(y | \mathbf{x})$ is α -Hölder as a map from $[0, 1]^{p+1}$ to \mathbb{R} for some $0 < \alpha \leq 2$. Additionally, we assume $\log p_0$ is d_0 -sparse in the sense that it depends on (y, \mathbf{x}) only through the coordinates in $S_0 \subseteq \{1, \dots, p+1\}$ where $|S_0| = d_0$, $d_0 = o(\log(n))$, and $d_0 \log p = o(n)$. Lastly, we assume that $\|f_0\|_\infty \lesssim \sqrt{\log n}$.

Remark 1. The assumption that $\log p_0$ is α -Hölder implies that p_0 is bounded and bounded away from 0. Condition F is used both to ensure that p_0 can be well-approximated with convolutions and to ensure that $\|f - f_0\|_\infty$ is small with sufficiently large prior probability.

Condition P (on Π) Let $S \subseteq \{1, \dots, p+1\}$ denote the coordinates of \mathbf{x} which the trees $f(\mathbf{x}, u)$ and $v(\mathbf{x}, u)$ split on.

- (P1) The support set S of (f, σ) has prior $\pi(S) = \binom{p+1}{|S|}^{-1} \pi_D(D)$ where $D \equiv |S|$ and $\pi_D(d)$ is an *exponentially decaying prior* satisfying $a_1(p+1)^{-a_3} \pi_D(d-1) \leq \pi_D(d) \leq a_2(p+1)^{-a_4} \pi_D(d-1)$ for some positive constants a_1, a_2, a_3, a_4 and $d = 1, \dots, p+1$.
- (P2) Given S , each tree $T_h, h = 1, \dots, m$ and $T_h^{(v)}, h = 1, \dots, m_v$ is assigned the branching process prior with splitting proportion $q(d) = \nu^d$ for some $\nu \in (0, 1/2)$.
- (P3) The leaf node parameters μ_{hl} of T_h are assigned independent $N(0, \sigma_\mu^2)$ priors.
- (P4) The log-variance function is given by $v(\mathbf{x}, u) = \xi + \sum_{h=1}^{m_v} g(\mathbf{x}, u; T_h^{(v)}, M_h^{(v)})$ where $e^{-\xi} \sim \text{Gam}(a_\sigma, b_\sigma)$ and $\mu_{hl}^{(v)} \stackrel{iid}{\sim} \pi_v$ where π_v is a strictly positive density supported on an interval $[-V, V]$.
- (P5) Splits in the tree ensemble can occur only at a number b_n of candidate split points $\mathcal{Z}_n \subseteq [0, 1]^{p+1}$, which are selected from uniformly. Additionally, $\log b_n \lesssim \log n$.
- (P6) For each n there exists a decision tree \hat{T} and leaf node values \hat{M} built from the candidate split-points in \mathcal{Z}_n such that the regression tree $f^*(\mathbf{x}, u) = g(\mathbf{x}, u; \hat{T}, \hat{M})$ satisfies $\|f_0 - f^*\|_\infty \lesssim (\log n/n)^{\beta/(2\beta+d_0)}$ where $\beta = \min\{\alpha, 1\}$.

Remark 2. Though P4 constrains the support of π_v , ξ is unbounded, allowing the variance function to have arbitrary scale even as the trees grant arbitrary flexibility in its shape.

Remark 3. The only assumption which is seemingly beyond our direct control is P6, which asserts that f_0 can be uniformly approximated with a single decision tree using the candidate split points \mathcal{Z}_n . Jeong and Rockova [2020] give several valid configurations of split points for which P6 would hold; for example, when \mathcal{Z}_n is a regular grid of size $b_n \asymp n^{cp}$ for c a sufficiently large constant if Condition F holds.

Under these assumptions, we have the following theorem:

Theorem 2. *Assume that Condition F and Condition P hold. Then, there exists a positive constant M such that $\Pi\{h(p_0, p_{f,\sigma}) \geq M\epsilon_n \mid \mathcal{D}_n\} \rightarrow 0$ in F_0 -probability, where $\epsilon_n = (n/\log n)^{-\frac{\alpha}{\alpha+1} \times \frac{\beta}{2\beta+d_0}} + \sqrt{d_0 \log(p+1)/n}$, where $\beta = \min\{\alpha, 1\}$.*

Remark 4. The gap between what is attainable by DR-BART-LH is larger than might be expected, as the rate is removed by a factor of $\alpha/(\alpha + 1)$ from the minimax rate. The reason this occurs is that Condition F implies $f_0(\mathbf{x}, u)$ has Hölder smoothness of $\alpha + 1 > 1$ in u , whereas BART is not known to be able to adapt to smoothness levels higher than 1. If we modify Condition F to state that $f_0(\mathbf{x}, u)$ is $\alpha + 1$ -smooth as a function of (u, \mathbf{x}) (as opposed to just in u) then it is possible to show that replacing the BART model with the SBART model of Linero and Yang [2018] gives the rate $n^{\alpha/(2\alpha+d_0)} \log(n)^{-\alpha(d_0+1)/(2\alpha+d_0)} + \sqrt{d_0 \log(p+1)/n}$ adaptively over α and S_0 for $\alpha \in (0, 2]$; extending these results to higher α using results of Plummer et al. [2021] is deferred to future work.

As argued by Li et al. [2020], the posterior rate of convergence is (bounded by) a sequence ϵ_n with $n\epsilon_n^2 \rightarrow \infty$ if we can find positive constants C_1, \dots, C_4 such that, for every sufficiently large n , there exists a set \mathcal{G}_n of conditional densities satisfying the following:

- (G1) $\Pi\{p_{f,\sigma} \in \text{KL}_{p_0}(C_1\epsilon_n)\} \geq \exp\{-C_2n\epsilon_n^2\}$, with $\text{KL}_{p_0}(\epsilon) = \{p : \text{KL}(p_0\|p), V(p_0\|p) \leq \epsilon^2\}$
- (G2) $\Pi(\mathcal{G}_n^c) \leq C_3 \exp\{-(C_2 + 4)n\epsilon_n^2\}$.
- (G3) $\log N(\mathcal{G}_n, \bar{\epsilon}_n, h) \leq C_4n\epsilon_n^2$ where $\bar{\epsilon}_n$ is a constant multiple of ϵ_n and $N(\mathcal{G}_n, \epsilon, d)$ denotes the ϵ -covering number of \mathcal{G}_n with respect to d [see, e.g. Ghosal et al., 2000].

The following two lemmas proved in the course of establishing Theorems 2 and 5 of Jeong and Rockova [2020] play a key role in establishing our results. The first ensures the prior on f places sufficient mass around f_0 and is essential in establishing G1.

Lemma 1. *Suppose that Condition F and Condition P hold and let $\delta_n = (\log n/n)^{\beta/(2\beta+d_0)}$. Then for sufficiently large n we have*

$$-\log \Pi(\|f - f_0\|_\infty \leq \delta_n \mid S = S_0) \lesssim n\delta_n^2.$$

The second lemma ensures that the support of the BART prior is “small” in a suitable sense, allowing us to verify G2 and G3.

Lemma 2. *Let \mathcal{F} denote the collection of decision tree ensembles with m trees which (i) split on no more than d variables, (ii) have at most K leaf nodes per tree, (iii) have at most b_n candidate split points, and (iv) satisfy $\sup_{p,h} |\mu_{hl}| \leq U$. Then*

$$\log N(\mathcal{F}, \epsilon, \|\cdot\|_\infty) \lesssim d \log(p+1) + K \log \left(\frac{d^m b_n^m K U}{\epsilon} \right).$$

Finally, Lemma 3 connects $h(p, q)$, $\text{KL}(p\|q)$, and $V(p\|q)$ to the supremum norm.

Lemma 3. *Suppose that Condition F holds. Then there exists a constant C_{KL} independent of (n, p) such that, for sufficiently small ϵ , we have*

$$\text{KL}_{p_0}(C_{\text{KL}}\epsilon) \supseteq \{\sigma(\mathbf{x}, u) \equiv \sigma \text{ is constant}, \sigma \in (\epsilon^{1/\alpha}, 2\epsilon^{1/\alpha}), \|f - f_0\|_\infty \leq \epsilon^{1+1/\alpha}\}.$$

Additionally, for any bounded measurable functions $f_1, f_2, \log \sigma_1, \log \sigma_2 : [0, 1]^{p+1} \rightarrow \mathbb{R}$:

$$h(p_{f_1, \sigma_1}, p_{f_2, \sigma_2}) \lesssim \sqrt{\|\log \sigma_1 - \log \sigma_2\|_\infty} + \frac{\|f_1 - f_2\|_\infty}{\inf_{\mathbf{x}, u} \sigma_1(\mathbf{x}, u) \wedge \sigma_2(\mathbf{x}, u)}.$$

Straightforward application of Lemmas 1 – 3 suffices to verify G1 – G3. The first part of Lemma 3 allows us to decompose the probability of the KL ball in G1 into pieces that can be bounded by Lemma 1. To verify G2, we consider a sieve defined by individual sieves for f , v , and ξ ; the second part of Lemma 3 allows us to bound the Hellinger distance between a conditional density and an element in this sieve and Lemma 2 then ensures that the entropy is appropriately bounded. Given the sieve, G3 follows given Condition P.

5 Simulations

Here, we evaluate how well DR-BART and other methods estimate conditional densities and appropriately express uncertainty about these estimates. We do so via variants of a challenging univariate example. Additional simulation details can be found in the Supplement.

5.1 Simulation 1: Contrasting DR-BART Models

Here, we introduce our basic simulation setup and gain insight into the differences between DR-BART-L, DR-BART-LH, and the full DR-BART model, before comparing to other methods. We consider a challenging example with a single regressor:

$$X_i \stackrel{iid}{\sim} U(0, 1), Y_i = f_0(X_i) + \epsilon_i(X_i) \quad (22)$$

where

$$f_0(\mathbf{x}) = 5 \exp[15(x - 0.5)] / (1 + \exp[15(x - 0.5)]) - 4x$$

and $\epsilon_i(X_i)$ is given by

$$p(\epsilon | X = x) = \lambda(x)N(\epsilon; 2x - 0.6, 0.3^2) + (1 - \lambda(x))p_G(\exp(\epsilon), 0.5 + x^2, 1.0) \exp(\epsilon),$$

where $\lambda(x) = \exp[-10(x - 0.8)^2]$ and the second component of $p(\epsilon | x)$ is a log-Gamma distribution with scale 1 and shape $0.5 + x^2$. Figure 3 shows selected quantile processes and conditional densities. The log-Gamma component is skewed and heteroscedastic, and the normal component is much more concentrated. The conditional distributions are nearly all unimodal, but for x values around 0.4 – 0.6 the density is quite peaked around the mode with a heavy left tail. At $x = 0.8$, ϵ has exactly a $N(1, 0.3^2)$ distribution.

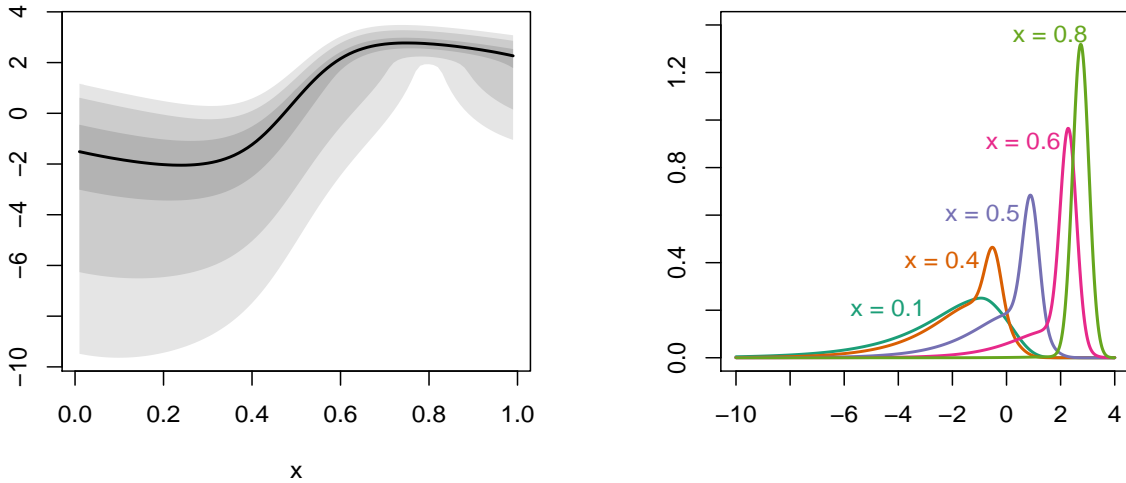


Figure 3: (Left) Conditional quantiles of the example in Section 5. Bands are equal-tailed 98%, 90%, and 50% intervals as a function of x . The solid line is the median process. (Right) The conditional pdf for selected x values.

Representative results for a single dataset are shown in Figure 4, which shows the estimated predictive density at $x = 0.1, 0.5, 0.8$. All three models do well when $x = 0.8$; BART captures the nonlinear mean function particularly well since the noise is low and symmetric, and the variance is well-estimated since a peak of approximately this width is present in many of the conditional densities. However, DR-BART-L predictably struggles at $x = 0.1$ when the peak disappears and the density becomes much more diffuse and skewed. Some of this severe multi-modality can be mitigated by adjusting the prior to include more / larger trees. But the fundamental problem is with the single bandwidth parameter: it must be low to capture the peak, which means that the spread in $p(y|x = 0.1)$ has to be captured by $f(0.1, u)$ varying greatly in u , yielding rougher densities.

DR-BART-LH and DR-BART perform much better, with the full model doing slightly better, particularly when $x = 0.1$, since it is a location-scale mixture and can capture the long left tail by splitting on u in the variance function to add high-variance “components”. The differences are fairly modest though, and the increase in computation time is $\sim 25\%$. Given its comparable performance, DR-BART-LH is a viable alternative to the full model, especially when most of the conditional densities are not severely multimodal or skewed.

5.2 Competing Methods

We now compare the full DR-BART model to a variety of other methods for conditional density estimation. First, we compare to the Probit Stick-Breaking Process Mixture (PSBPM) in Chung and Dunson [2012]. Chung et al. model the

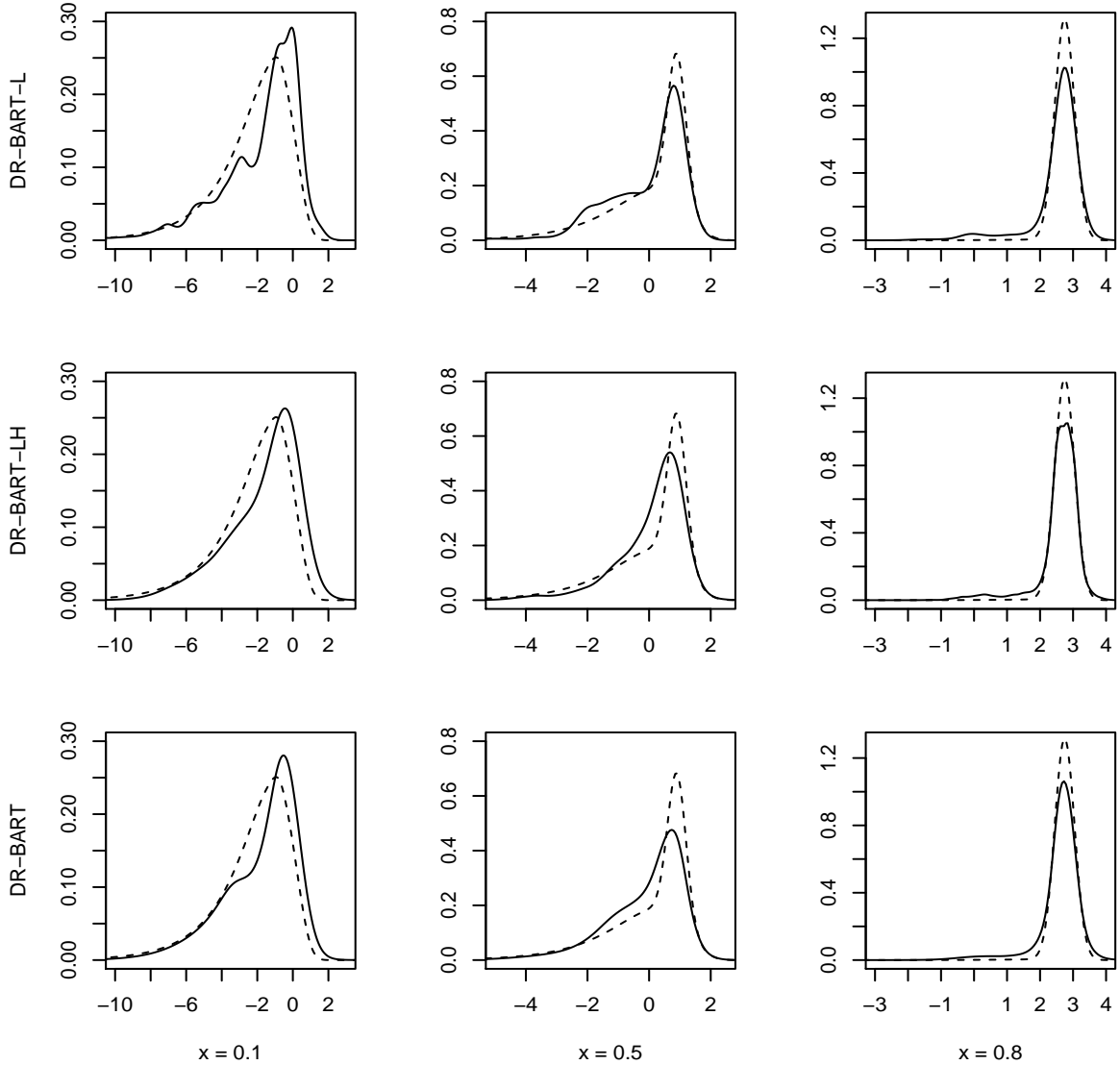


Figure 4: Representative true (dotted) and estimated (solid) densities from Simulation 1.

conditional density $p(y|\mathbf{x})$ via an infinite mixture of normal linear regressions according to mixing distributions $P_{\mathbf{x}}$:

$$p(y|\mathbf{x}) = \int \phi_{\tau}(y - \mathbf{x}'\beta) dP_{\mathbf{x}}$$

where the prior over the $P_{\mathbf{x}}$ is defined by a covariate-dependent stick-breaking prior.

Second, we compare to the Soft BART Density Sampler (**SBART-DS**) of Li et al. [2020] which models conditional densities by modulating a base model $h(y|\mathbf{x}, \theta)$ via a link function $\Phi(\mu) : p(y|\mathbf{x}, \theta) \propto h(y|\mathbf{x}, \theta)\Phi\{r(y, \mathbf{x})\}$. There are many possible choices for h , r , and Φ ; Li et al. choose to center their conditional densities on a normal linear regression: $h(y|\mathbf{x}, \theta) = \phi_{\sigma_{\theta}}(y - \mathbf{x}'\beta_{\theta})$ and Φ to be a probit link. They take r to be the weighted sum of Soft Additive Regression Trees [Linero and Yang, 2018] with random Fourier expansions approximating a Gaussian process in the leaf nodes, as in Starling et al. [2020].

Third, we compare to a Dirichlet Process Mixture Model (**DPMM**) of Jara et al. [2011] that models (\mathbf{x}, y) as jointly normal and computes the implied conditional of y on \mathbf{x} .

Lastly, we compare to a generalization of Zhou et al. [2017] that incorporates covariates into the transfer function μ , which has a Gaussian process prior (**DR-GP**). This approach is similar to ours in its use of a latent u to perform

conditional density estimation. It differs in its use of 1. a Gaussian process to map (u, \mathbf{x}) to the observed response and 2. a homoscedastic, inverse Gamma prior on σ , instead of our BART priors on each.

5.3 Simulation 2: Univariate Example

Here, we consider the same simulation as above. We simulate $n = 800$ data points from model (22) and fit all methods. Fits and credible intervals for a representative simulation are shown in Figure 5. We see that DR-BART estimates the mean well with appropriate uncertainty quantification across all conditional densities, though it struggles to fully capture the peak of the normal density at $x = 0.8$ given how concentrated it is. Most the other methods are able to fit the densities at $x = 0.1$ and $x = 0.8$ reasonably well, but have difficulty with capturing both the peak and strong skew present in $p(y | x = 0.5)$. Results aggregated across 100 simulations are shown in Table 1. As suggested by Figure 5, DR-BART outperforms all other methods when $x \in \{0.1, 0.5\}$, but falls short of always capturing the peak at $x = 0.8$. DPMM estimates $p(y | x = 0.8)$ particularly well, which is to be expected given that it is built upon a normal specification.

We next assess how well the 95% credible bands of each method cover the true $p(y | x)$. Table 1 also displays the proportion of simulations where the credible bands fully contain the true density within the true 95% HDR interval. As Figure 5 suggests, DR-BART is able to do so consistently for $x = 0.1$ and $x = 0.5$, but not always for $x = 0.8$. For this and the next two simulations, the Supplement also contains information on credible band width and predictive coverage, which was consistently close to nominal for all methods but PSBPM.

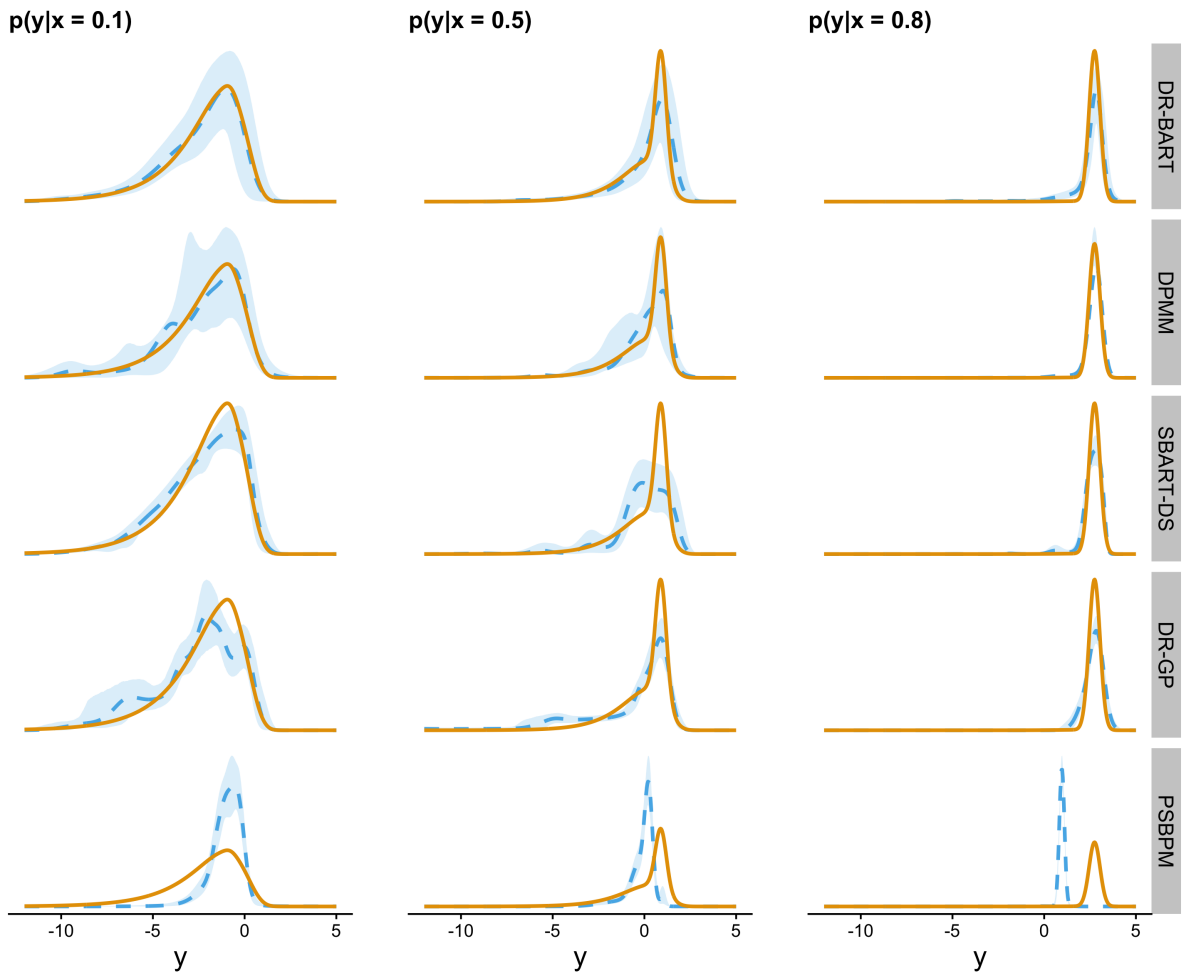


Figure 5: Representative true (solid) and estimated (dashed) densities from Simulation 2.

5.4 Simulation 3: Irrelevant Covariates

Here, we generate data as above, but supply an additional 14 irrelevant, uniformly distributed variables, with pairwise correlations of 0.3, to each method. For each method, we evaluate the predictive density with the irrelevant variables fixed to 0.5. Figure 6 and Table 2 illustrate the results. While the quality of DR-BART’s fit decreases, it compensates by increasing the width of its credible bands to capture the truth. DPMM and DR-GP, which in the previous simulation fit better at $x = 0.1, 0.8$ do not, however, adjust their estimates of uncertainty to counter the substantial degradation in their fits. Perhaps most notable is that DR-BART still has good pointwise coverage, whereas the other methods are overconfident in their overfitting to the irrelevant covariates. We also note that the SBART-DS credible bands are not more erratic than in Simulation 1, reflecting BART’s ability to perform variable selection.

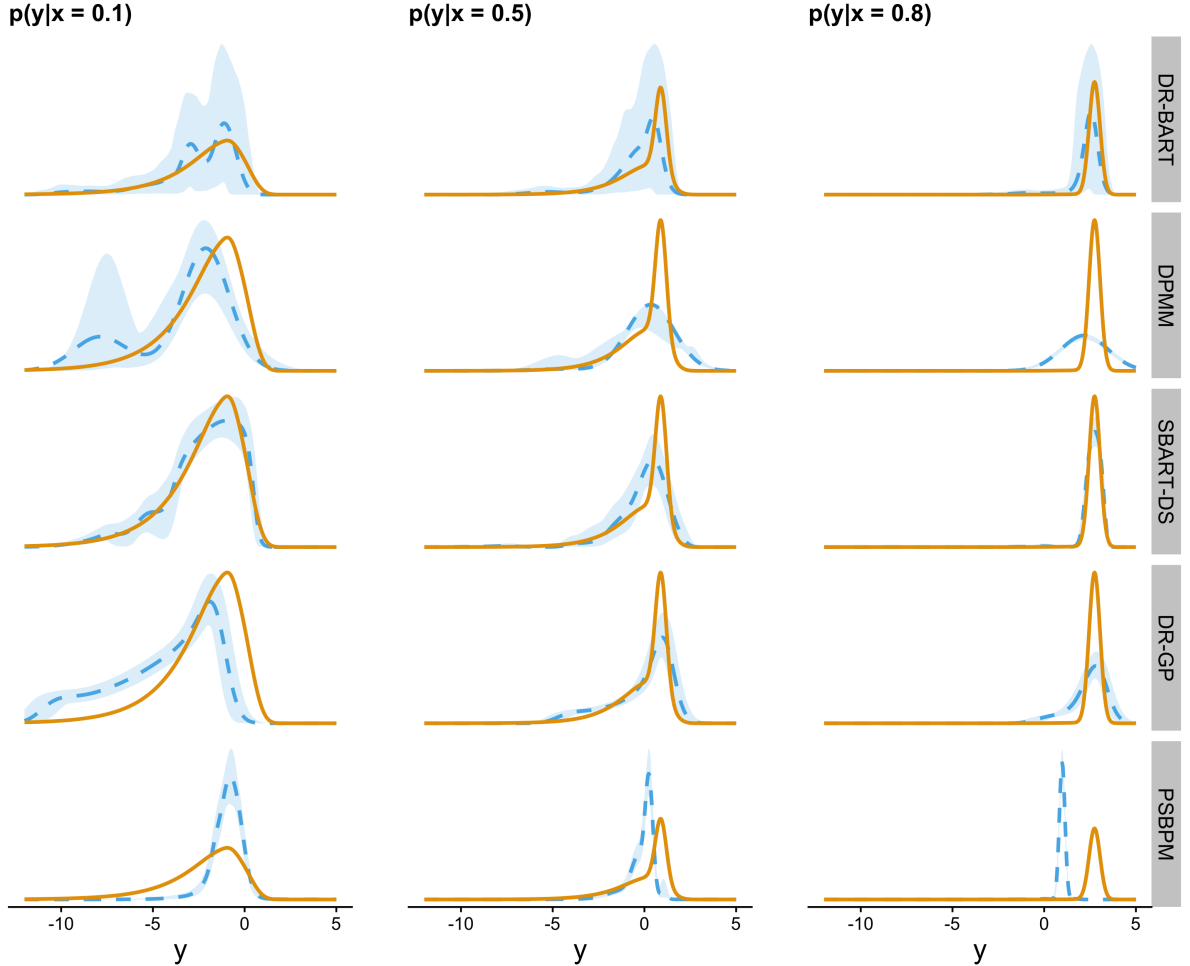


Figure 6: Representative true (solid) and estimated (dashed) densities from Simulation 3.

| | DR-BART | | DPMM | | SBART-DS | | DR-GP | | PSBPM | |
|-----------|---------|----------|-------|----------|----------|----------|-------|----------|-------|----------|
| | ERROR | COVERAGE | ERROR | COVERAGE | ERROR | COVERAGE | ERROR | COVERAGE | ERROR | COVERAGE |
| $x = 0.1$ | 1 | 0.93 | 1.67 | 0.75 | 1.65 | 0.48 | 2.74 | 0.02 | 9.80 | 0.00 |
| $x = 0.5$ | 1 | 0.61 | 1.01 | 0.62 | 2.20 | 0.00 | 1.46 | 0.00 | 2.14 | 0.00 |
| $x = 0.8$ | 1 | 0.19 | 0.28 | 0.85 | 0.79 | 0.00 | 1.03 | 0.00 | 2.27 | 0.00 |

Table 1: Error and Coverage for Simulation 2. Error is Wasserstein distance between true and estimated densities (normalized at each x for interpretability), averaged over 100 simulations. Coverage is the proportion of simulations in which 95% credible bands cover the truth within the true 95% HDR region.

| | DR-BART | | DPMM | | SBART-DS | | DR-GP | | PSBPM | |
|-----------|---------|----------|-------|----------|----------|----------|-------|----------|-------|----------|
| | ERROR | COVERAGE | ERROR | COVERAGE | ERROR | COVERAGE | ERROR | COVERAGE | ERROR | COVERAGE |
| $x = 0.1$ | 1 | 0.78 | 1.10 | 0.00 | 0.78 | 0.46 | 2.63 | 0.00 | 5.58 | 0.00 |
| $x = 0.5$ | 1 | 0.94 | 2.96 | 0.00 | 1.97 | 0.00 | 2.23 | 0.00 | 1.97 | 0.00 |
| $x = 0.8$ | 1 | 1.00 | 1.60 | 0.00 | 0.56 | 0.02 | 2.52 | 0.00 | 1.70 | 0.00 |

Table 2: Error and Coverage for Simulation 3. Error is Wasserstein distance between true and estimated densities (normalized at each x for interpretability), averaged over 50 simulations. Coverage is the proportion of simulations in which 95% credible bands cover the truth within the true 95% HDR region.

5.5 Simulation 4: Insufficient Data

Next, we explore the ability of DR-BART to appropriately express uncertainty about conditional distributions in regions of x -space where there is little data. To do so, we simulate y given x as in the previous experiments; however, instead of simulating x uniformly, we simulate it from a mixture of uniforms: $0.475 \times U_{[0,0.4]} + 0.05 \times U_{[0.4,0.6]} + 0.475 \times U_{[0.6,1]}$, where $U_{[a,b]}$ denotes the density of a $U(a, b)$ random variable. With only 5% of the mass lying between $x = 0.4$ and $x = 0.6$, estimation of $p(y | x = 0.5)$ is much harder. With this experiment, we expect the performance of all methods to degrade; we are interested in whether their uncertainty grows appropriately to account for the lack of data.

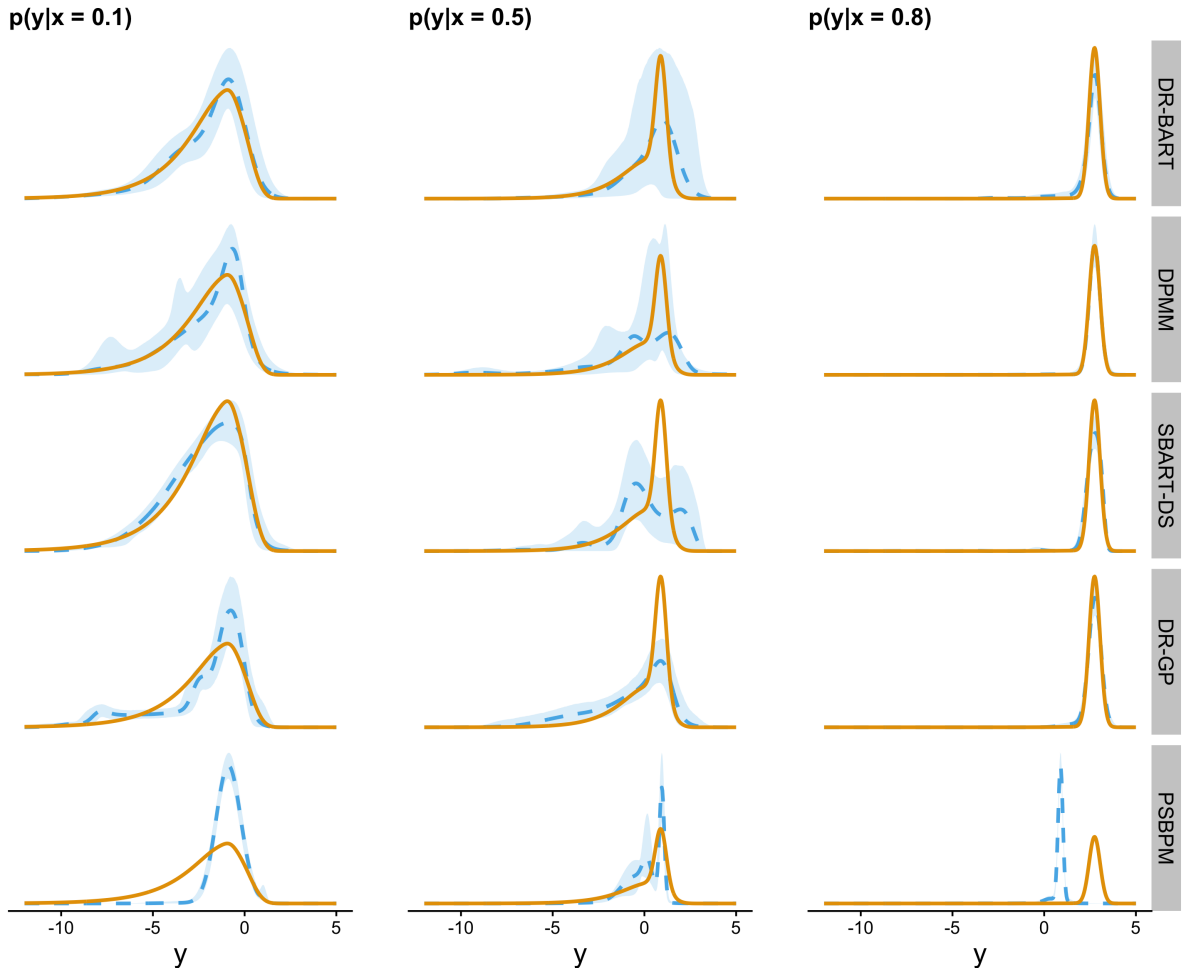


Figure 7: Representative true (solid) and estimated (dashed) densities from Simulation 4.

Figure 7 shows a representative simulation. Most of the methods perform better in estimating $p(y | x = 0.8)$, as there is now substantially more data in that region of the space. At $x = 0.5$, only DR-BART and DPMM increase their

| | DR-BART | | DPMM | | SBART-DS | | DR-GP | | PSBPM | |
|-----------|---------|----------|-------|----------|----------|----------|-------|----------|-------|----------|
| | ERROR | COVERAGE | ERROR | COVERAGE | ERROR | COVERAGE | ERROR | COVERAGE | ERROR | COVERAGE |
| $x = 0.1$ | 1 | 0.96 | 1.55 | 0.94 | 1.59 | 0.36 | 2.87 | 0.02 | 10.35 | 0.00 |
| $x = 0.5$ | 1 | 0.54 | 1.34 | 0.56 | 1.91 | 0.02 | 1.34 | 0.00 | 1.26 | 0.00 |
| $x = 0.8$ | 1 | 0.16 | 0.29 | 0.80 | 0.79 | 0.02 | 1.01 | 0.00 | 2.69 | 0.00 |

Table 3: Error and Coverage for Simulation 4. Error is Wasserstein distance between true and estimated densities (normalized at each x for interpretability), averaged over 50 simulations. Coverage is the proportion of simulations in which 95% credible bands cover the truth within the true 95% HDR region.

| | $a = 0$ | | $a = 1$ | | $a = 5$ | | $a = 15$ | | $a = 25$ | | $a = 35$ | |
|-----------|---------|------|---------|------|---------|------|----------|------|----------|------|----------|------|
| | DR-B | S-DS | DR-B | S-DS | DR-B | S-DS | DR-B | S-DS | DR-B | S-DS | DR-B | S-DS |
| $x = 0.1$ | 0.39 | 0.56 | 0.20 | 0.55 | 0.37 | 0.50 | 0.39 | 0.62 | 0.82 | 0.97 | 0.37 | 1.04 |
| $x = 0.5$ | 0.76 | 1.09 | 0.74 | 0.85 | 0.89 | 0.91 | 0.39 | 1.50 | 0.71 | 1.57 | 0.80 | 2.20 |
| $x = 0.8$ | 1.11 | 0.94 | 1.32 | 0.96 | 1.05 | 1.31 | 1.05 | 2.53 | 1.26 | 2.90 | 1.04 | 3.25 |

Table 4: Wasserstein distance between true, estimated densities in Simulation 5, averaged over 50 simulations. As a increases and the true mean becomes increasingly nonlinear, SBART-DS (S-DS) is hindered by its reliance on a linear base model, while DR-BART (DR-B) is unaffected.

uncertainty in their estimation; the other methods have relatively poor fits with insufficient uncertainty about them. Table 3 summarizes this information across 50 simulations. DR-BART performs better in predicting $p(y | x = 0.5)$, but the relative performance for $x \in \{0.1, 0.8\}$ is comparable to that in Section 5.3. Table 3 also supports the observation that DR-BART and DPMM are unique in increasing the uncertainty in their estimates in response to the lack of data.

5.6 Simulation 5: Comparison of BART Models

Here, we further compare DR-BART to SBART-DS. Because both are built off of (S)BART models, we expect them to share many desirable properties, such as high flexibility and the ability to identify interaction effects and perform variable selection. SBART-DS, however, is centered on a base model, which may degrade the fit when the truth is far from the base model. Furthermore, there are cases in which prior information suggesting a reasonable base model may be lacking. To explore reliance on the base model, we run the original univariate simulation, but change the mean to be $f_0(x) = a(x - 0.5)^2$. For small a , the mean is approximately linear for $x \in [0, 1]$, as specified by SBART-DS. But as a increases, it becomes increasingly nonlinear and we expect performance to degrade. Using $n = 1500$, we run 50 simulations for each $a \in \{0, 1, 5, 15, 25, 35\}$, summarized in Table 4. For small a , both methods perform well. But the increasing nonlinearity of the mean as a increases hinders SBART-DS' performance deteriorates, while DR-BART is unaffected.

6 Applications

We consider two applications of DR-BART. In both cases, we fit DR-BART-LH; the full DR-BART model gave similar results since both applications involve fairly well-behaved densities. For all models, σ_0^2 is set to be half the standard deviation of the OLS residuals and results seem to be insensitive to reasonable choices of this value. We also set $a_0 = \log(\sqrt{4})^{-2}$. For each model, 10,000 MCMC samples are collected after a burn-in of 10,000 iterations. The estimands of interest in both sections are functions of quantiles; we will use $Q(s | \mathbf{x})$ to denote the quantile function of $P(y | \mathbf{x})$.

6.1 Calculating Student Growth

We consider the estimation of student growth from a series of test scores, using anonymized mathematics test scores provided in the SGP R package [Betebenner et al., 2011]. Castellano and Ho [2013] gives an overview of current mean and quantile regression approaches to this problem, as well as some consideration to the substantive problem of measuring student growth. Statistically, the problem reduces to estimating a series of conditional densities $p(y_t | y_{t-1}, y_{t-2}, \dots, y_0)$. These distributions are heteroscedastic and tend to become skewed as they approach the extremes. The current state of the art is the quantile regression methodology implemented in the SGP package and detailed in

Betebenner [2009]. The quantile regression models are specified as

$$Q_{y_t}(s | y_{t-1}, \dots, y_0) = \sum_{r=0}^{t-1} \eta_r^{(s)}(y_r). \quad (23)$$

where each function $\eta_r^{(s)}(\cdot)$ is given a B-spline basis expansion. This model is fit at each of the 99 percentiles to approximate the conditional distribution. This procedure does not yield valid estimates for percentiles of the conditional distribution in general, due to quantile crossing (though this can be corrected post-hoc [Chernozhukov et al., 2010]). Assessing uncertainty in this framework is challenging as well, and analysis generally relies solely on point estimates. Bayesian density regression addresses both problems simultaneously.

We fit independent DR-BART-LH models to scores from grades 4-7, each conditional on all the previous scores as well as the grade 3 scores. For simplicity we took a subsample of 3,000 students with complete data from grades 3-7. An interesting feature of this data is the interactions between previous test scores on the predictive distributions. One mechanism for this is regression to the mean: large jumps in test scores are unlikely to be sustained. Figure 8 gives an example, displaying posterior predictive densities for grade 5 scores when fixing grade 3 and 4 scores at all combinations of their marginal quartiles. In the absence of interactions the shift between the pairs of solid and dashed densities would be equal. Figure 9 further suggests the presence of an interaction effect. When $y_4 = 455$, y_3 has a smaller effect on the quantiles of $p(y_5 | y_4, y_3)$ than when $y_4 = 538$. Note that the additive model in (23) cannot capture such an interaction and requires the curves to be equal.

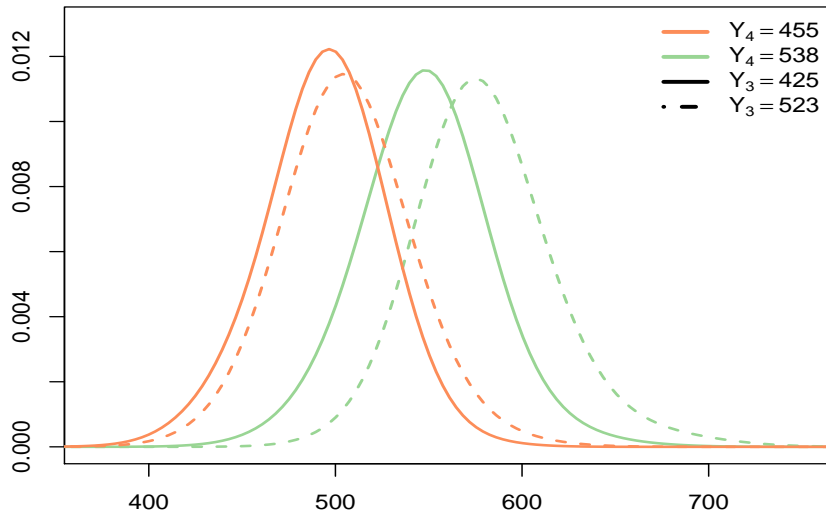


Figure 8: Four posterior predictive distributions for grade 5 scores obtained by setting grade 3 and 4 scores at each combination of their marginal quartiles. The effect of the grade 3 score on the predictive distribution clearly depends on the value of the grade 4 score, an important interaction that DR-BART is well-equipped to capture.

A key objective in student growth modeling is computing growth quantile targets. A growth quantile is a quantile of the predictive distribution for the current test score given the score history. Intuitively, it provides a measure of how well a student performed on the test relative to academic peers (the hypothetical population of students with identical test history). A growth quantile target is the level of consecutive quantile growth that would be required to achieve pre-established achievement targets. For these data, there are four achievement levels used to define achievement targets: Unsatisfactory, Partially Proficient, Proficient, or Advanced. Growth quantile targets answer questions like “What level of sustained growth is necessary for a student with grade 3 test score y_3 to be Proficient by grade 7?”. This is different than simulating score trajectories and computing the probability that a student reaches a target. Growth quantile targets are intended to promote a “what will it take” attitude over a fatalistic “where will s/he be” attitude [Betebenner, 2011].

The current methodology for computing growth quantile targets uses a series of point estimates, ignoring uncertainty in the quantile curve estimates. But this uncertainty is generally not negligible, particularly for students with extreme test scores. To illustrate, we computed posterior samples of growth quantile curves for a hypothetical third grade student who scored at the cusp of Unsatisfactory/Partially Proficient on the third grade math test. Figure 10 plots this student’s

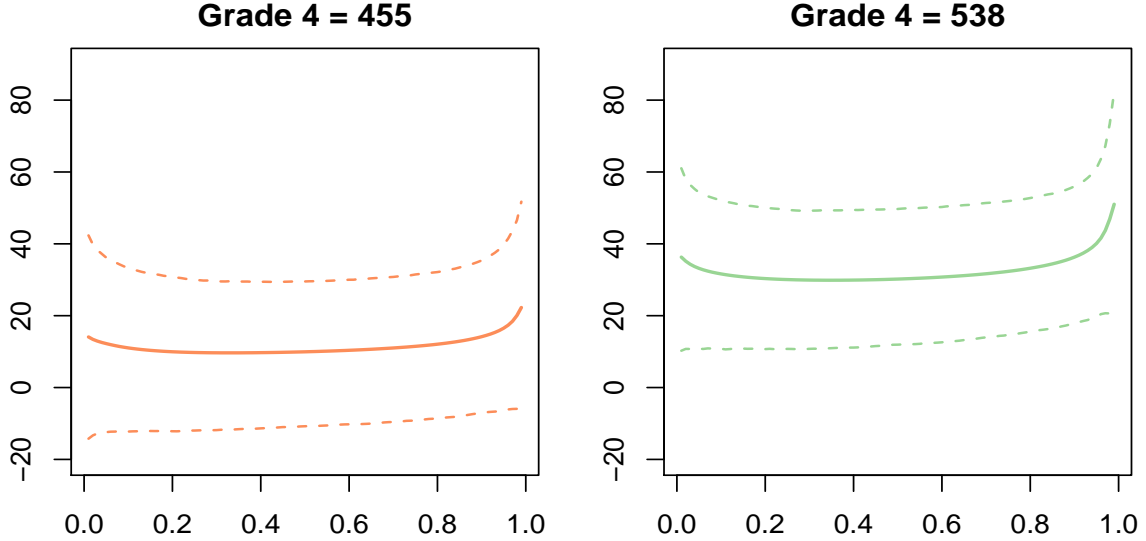


Figure 9: Quantile effects $Q_{y_5}(s | y_4, y_3 = 523) - Q_{y_5}(s | y_4, y_3 = 425)$ for $y_4 = 455, 538$ along with 90% credible intervals. Under Betebenner [2009]’s additive model these two curves are forced to be equal. This reveals a likely interaction between grade 3 and grade 4 scores: the posterior mean of the 538 curve is nearly outside the 455 credible interval.

growth quantile curves and 90% credible intervals for grades 4-7. It is easy to read off growth quantile targets from these charts: For example, the bottom right panel of Figure 10 shows that if the student sustains 60th percentile growth in grades 5,6 and 7, there is a 95% probability of remaining partially proficient in grade 7. Having a 50% chance of reaching proficiency in grade 7 would require sustained growth at the 80th percentile, which is probably unattainable without some new intervention. Similar curves can be computed starting with any grade and any score history.

In particular, we analyze a subset of public use microdata from the U.S. Census, originally compiled by Angrist et al. [2006] to estimate returns to education across the income distribution. For the 1980, 1990 and 2000 samples they extracted all U.S. born white and black men aged 40-49 with positive annual earnings and positive hours worked in the year prior to the Census. Records with imputed values were excluded, and wages were adjusted to 1989 dollars. Angrist et al. [2006] and its supplementary materials contain details of how the data were obtained and cleaned. The response is log monthly wages, and the covariates include years of education, experience (defined as $age - education - 12$) and race (white or black). The study objective was to estimate returns to education as a function of quantile index. Taking Q as the quantile function of wages, the return to education at quantile index s is

$$100 \times \frac{Q(s | \mathbf{x}_2) - Q(s | \mathbf{x}_1)}{Q(s | \mathbf{x}_1)}, \quad (24)$$

the predicted percentage change in monthly wage from modifying education in \mathbf{x}_1 to yield \mathbf{x}_2 . While Angrist et al. [2006] fit a linear quantile regression to estimate the effect of each additional year of education, we fit DR-BART-LH to each census sample separately, subsampling 5000 units from each, and study the difference between 12 and 16 years of education. In general the effect of a single additional year of schooling is probably heterogenous. For example, the difference in earnings between 11 and 12 years of schooling should be larger than the difference between 10 and 11, because 12 years of education in the U.S. typically indicates that the respondent completed high school. BART readily accommodates non-smooth features in the regression function, while usual econometric analyses assume that regression functions are linear or quadratic in education (or experience).

Figure 11 shows the return to education for a 45 year old white male, comparing 12 to 16 years of schooling. In 1990, returns were highest at low and high quantiles, whereas in 2000 the returns are actually increasing as a function of the quantile index. Other covariate vectors show similar patterns, although the exact estimates vary (and are somewhat unstable for black men due to small sample size). Angrist et al. [2006] found a similar pattern in the returns at the population level and verified it using additional data from the Current Population Survey, so this seems to be a robust finding.

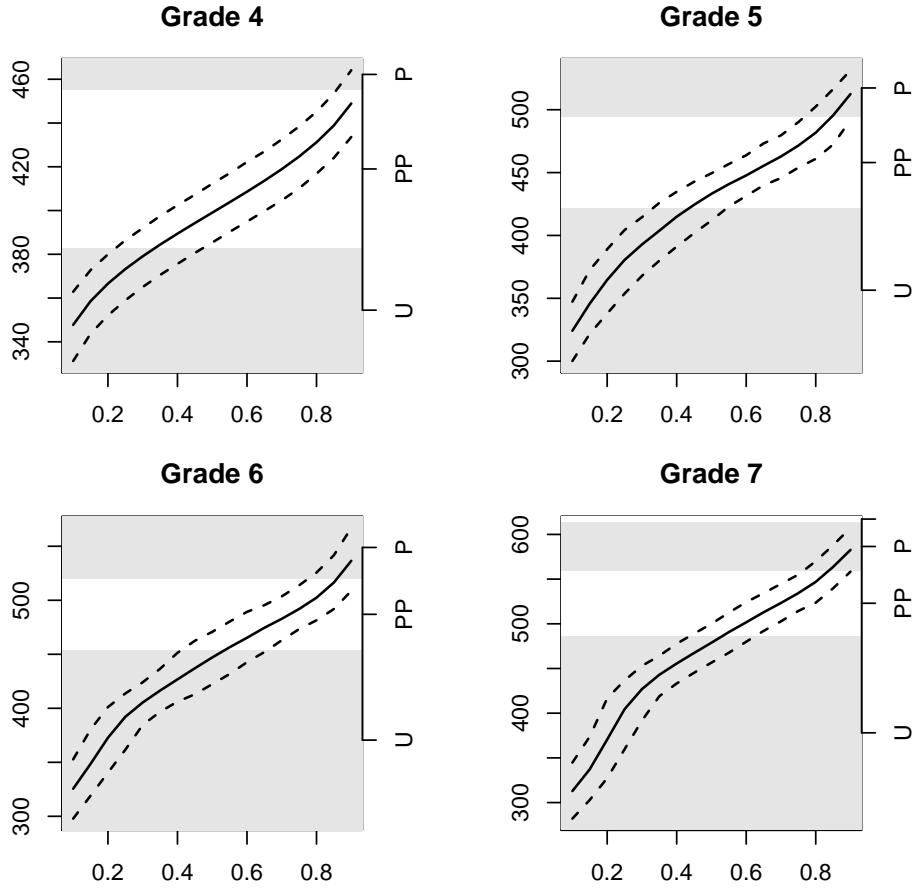


Figure 10: Projected scores as a function of quantile growth for a student at the cusp of Unsatisfactory/Partial Proficiency in grade three. The solid line is the posterior mean and dashed lines are pointwise 90% credible intervals. Shaded regions correspond to achievement thresholds: Unsatisfactory (U), Partially Proficient (PP), Proficient (P).

7 Conclusion

In this paper, we introduced a new nonparametric model, DR-BART, extending Bayesian Additive Regression Trees to the novel and challenging setting of density regression. This model has the appeal of being flexible yet easy to specify and understand, with few prior parameters to set. This distinguishes DR-BART from other nonparametric Bayesian methods for density regression, which often include collections of infinite dimensional regression parameters. Inference via MCMC is fast, with acceptable mixing in our examples obtained in a matter of minutes for datasets with thousands of observations. We showed DR-BART to empirically outperform a variety of other density regression methods in its ability to point estimate conditional densities and to express uncertainty about these estimates. Lastly, we extended previous work on posterior concentration results for BART and for density estimation via a latent variable model to prove concentration rates for DR-BART.

Having introduced the latent variable as a modeling device a natural question is whether it might represent some real structure in the scientific problem, like measurement error in \mathbf{x} , some combination of omitted variables, or a latent construct like ability or motivation. Any of these seem plausible in the applications presented here. In the educational testing application we treated the latent variables as independent. This is a useful “saturated” model for the joint distribution of test scores, but models for dependence across these variables or lower-dimensional representations based on shared latent variables may be more scientifically meaningful or efficient. Further modeling of latent variables within BART is a promising area for future work, even beyond the setting of density regression.

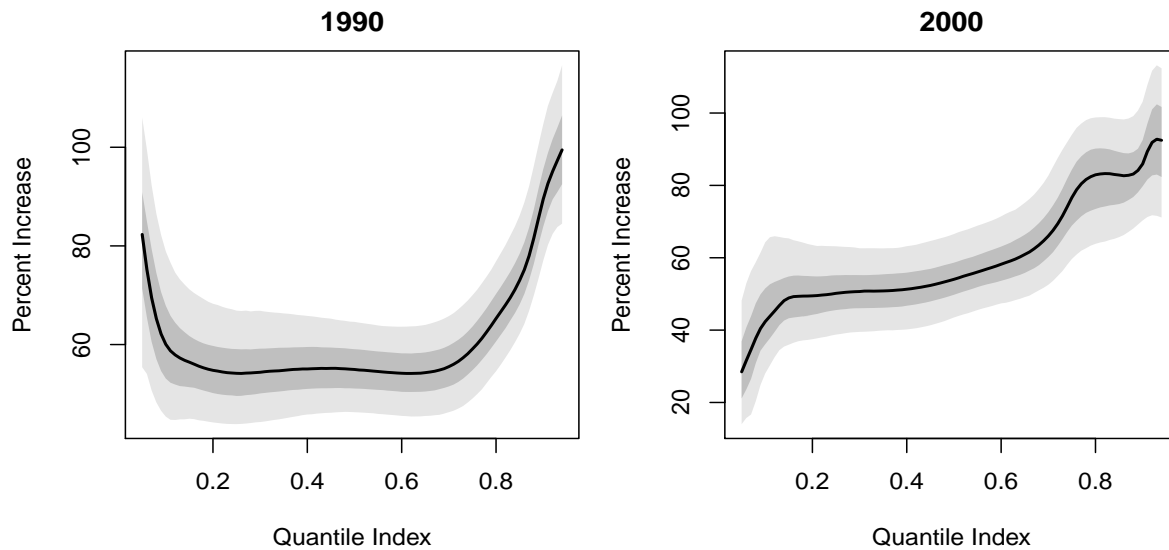


Figure 11: Returns to education (16 years versus 12 years) for a 45 year old white man.

References

- D. Wittman. What Lies Beneath: Using $p(z)$ To Reduce Systematic Photometric Redshift Errors. *The Astrophysical Journal*, 700(2):L174–L177, jul 2009.
- George Karabatsos and Stephen G. Walker. Bayesian unimodal density regression for causal inference. Technical report, Society for Research on Educational Effectiveness, May 2011.
- Tilmann Gneiting and Matthias Katzfuss. Probabilistic forecasting. *Annual Review of Statistics and Its Application*, 1: 125–151, 2014.
- Dan A. Black, Jose Galdo, and Jeffrey A. Smith. Evaluating the worker profiling and reemployment services system using a regression discontinuity approach. *The American Economic Review*, 97(2):104–107, 2007. ISSN 00028282.
- Joseph B. Kadane and Surya T. Tokdar. Simultaneous Linear Quantile Regression: A Semiparametric Bayesian Approach. *Bayesian Analysis*, 7(1):51 – 72, 2012. doi:10.1214/12-BA702.
- Maxime Sanguier, Olivier Fercoq, and d’Alché Buc Florence. Joint Quantile Regression in Vector-Valued RKHSs. In *Advances in Neural Information Processing Systems*, 2016.
- Victor Chernozhukov, Iván Fernández-Val, and Alfred Galichon. Quantile and probability curves without crossing. *Econometrica*, 78(3):1093–1125, 2010.
- Michael Gerfin. Income distribution, income inequality and life cycle effects - a nonparametric analysis for Switzerland. *Swiss Journal of Economics and Statistics*, 130:509–522, 1994.
- Mary C. Daly and Robert G. Valletta. Inequality and poverty in United States: The effects of rising dispersion of men’s earnings and changing family behaviour. *Economica*, 73:75–98, 2006.
- Debdeep Pati, Anirban Bhattacharya, and David Dunson. Posterior Convergence Rates in Non-linear Latent Variable Models, 2011.
- S. Kundu and D. B. Dunson. Latent factor models for density estimation. *Biometrika*, 101(3):641–654, June 2014. ISSN 0006-3444. doi:10.1093/biomet/asu019.
- Shuang Zhou, Debdeep Pati, Anirban Bhattacharya, and David Dunson. Adaptive posterior convergence rates in non-linear latent variable models, 2017.
- A. R. Linero and Y. Yang. Bayesian regression tree ensembles that adapt to smoothness and sparsity. *Journal of the Royal Statistical Society: Series B*, 80(5), 2018.
- Damian W Betebenner, Adam VanIwaarden, Ben Domingue, Yi Shang, Jonathan Weeks, John Stewart, Jinnie Choi, Xin Wei, Hi Shin Shim, Xiaoyuan Tan, et al. SGP: An R package for the calculation and visualization of student growth percentiles & percentile growth trajectories. 2011.

- Joshua Angrist, Victor Chernozhukov, and Iván Fernández-Val. Quantile regression under misspecification, with an application to the US wage structure. *Econometrica*, 74(2):539–563, 2006.
- Robert A Jacobs, Michael I Jordan, Steven J Nowlan, and Geoffrey E Hinton. Adaptive mixtures of local experts. *Neural Computation*, 3(1):79–87, 1991.
- Michael I Jordan and Robert A Jacobs. Hierarchical mixtures of experts and the em algorithm. *Neural computation*, 6(2):181–214, 1994.
- John Geweke and Michael Keane. Smoothly mixing regressions. *Journal of Econometrics*, 138(1):252–290, 2007.
- Mattias Villani, Robert Kohn, and Paolo Giordani. Regression density estimation using smooth adaptive Gaussian mixtures. *Journal of Econometrics*, 153(2):155–173, 2009.
- Andriy Norets et al. Approximation of conditional densities by smooth mixtures of regressions. *The Annals of Statistics*, 38(3):1733–1766, 2010.
- Debdeep Pati, David B Dunson, and Surya T Tokdar. Posterior consistency in conditional distribution estimation. *Journal of Multivariate Analysis*, 116:456–472, 2013.
- Andriy Norets and Justinias Pelenis. Posterior consistency in conditional density estimation by covariate dependent mixtures. *Econometric Theory*, 30(03):606–646, 2014.
- Andriy Norets and Debdeep Pati. Adaptive Bayesian estimation of conditional densities, 2014.
- P. Muller, A. Erkanli, and M. West. Bayesian curve fitting using multivariate normal mixtures. *Biometrika*, 83(1):67–79, March 1996. ISSN 0006-3444. doi:10.1093/biomet/83.1.67.
- Ju-Hyun Park and David B Dunson. Bayesian generalized product partition model. *Statistica Sinica*, 20(20):1203–1226, 2010.
- Mike West and Michael D Escobar. *Hierarchical priors and mixture models, with applications in regression and density estimation*. Duke University, 1993.
- Babak Shahbaba and Radford Neal. Nonlinear Models Using Dirichlet Process Mixtures. *The Journal of Machine Learning Research*, 10:1829–1850, December 2009. ISSN 1532-4435.
- Matthew A. Taddy and Athanasios Kottas. A Bayesian Nonparametric Approach to Inference for Quantile Regression. *Journal of Business & Economic Statistics*, 28(3):357–369, July 2010. ISSN 0735-0015. doi:10.1198/jbes.2009.07331.
- John Molitor, Michail Papathomas, Michael Jerrett, and Sylvia Richardson. Bayesian profile regression with an application to the National survey of children’s health. *Biostatistics*, 11(3):484–98, July 2010. ISSN 1468-4357. doi:10.1093/biostatistics/kxq013.
- Sara Wade, Silvia Mongelluzzo, and Sonia Petrone. An Enriched Conjugate Prior for Bayesian Nonparametric Inference. *Bayesian Analysis*, 6(3):359–385, 2011.
- David B Dunson and Abhishek Bhattacharya. Nonparametric Bayes Regression and Classification Through Mixtures of Product Kernels. In Jose M. Bernardo, M. J. Bayarri, James O. Berger, A. P. Dawid, David Heckerman, Adrian F. M. Smith, and Mike West, editors, *Proceedings of 9th Valencia International Conference on Bayesian Statistics*. Oxford University Press, 2011.
- Lauren A. Hannah, David M. Blei, and Warren B. Powell. Dirichlet Process Mixtures of Generalized Linear Models. *The Journal of Machine Learning Research*, pages 1923–1953, July 2011. ISSN 1532-4435.
- Sara Wade, DB Dunson, Sonia Petrone, and Lorenzo Trippa. Improving Prediction from Dirichlet Process Mixtures via Enrichment. *Journal of Machine Learning Research*, 15:1041–1071, 2014.
- Stephen G. Walker and George Karabatsos. Revisiting Bayesian curve fitting using multivariate normal mixtures. In Paul Damien, Petros Dellaportas, Nicholas G. Polson, and David A. Stephens, editors, *Bayesian Theory and Applications*. Oxford University Press, 01 edition, 3 2013. ISBN 9780199695607.
- Steven N MacEachern. Dependent nonparametric processes. In *ASA proceedings of the section on Bayesian statistical science*, pages 50–55, 1999.
- Steven N MacEachern. Dependent Dirichlet processes. *Unpublished manuscript, Department of Statistics, The Ohio State University*, 2000.
- Maria De Iorio, Peter Müller, Gary L Rosner, and Steven N MacEachern. An ANOVA model for dependent random measures. *Journal of the American Statistical Association*, 99(465):205–215, 2004.
- Jim E Griffin and MF J Steel. Order-based dependent Dirichlet processes. *Journal of the American Statistical Association*, 101(473):179–194, 2006.

- David B Dunson and Shyamal D Peddada. Bayesian nonparametric inference on stochastic ordering. *Biometrika*, 95(4): 859–874, 2008.
- Maria De Iorio, Wesley O Johnson, Peter Müller, and Gary L Rosner. Bayesian nonparametric nonproportional hazards survival modeling. *Biometrics*, 65(3):762–771, 2009.
- Lianming Wang and David B Dunson. Bayesian isotonic density regression. *Biometrika*, 98(3):537–551, 2011.
- Andrés F. Barrientos, Alejandro Jara, and Fernando A. Quintana. On the support of MacEachern’s dependent Dirichlet processes and extensions. *Bayesian Analysis*, 7(2):277–310, 06 2012. doi:10.1214/12-BA709.
- Hugh A. Chipman, Edward I. George, and Robert E. McCulloch. BART: Bayesian additive regression trees. *The Annals of Applied Statistics*, 4(1):266–298, March 2010. ISSN 1941-7330.
- Seonghyun Jeong and Veronika Rockova. The art of BART: On flexibility of Bayesian forests, 2020.
- Jared S Murray. Log-linear bayesian additive regression trees for multinomial logistic and count regression models. *Journal of the American Statistical Association*, pages 1–14, 2021.
- Stephen G. Walker. Sampling the Dirichlet Mixture Model with Slices. *Communications in Statistics - Simulation and Computation*, 36(1):45–54, January 2007. ISSN 0361-0918. doi:10.1080/03610910601096262.
- Maria Kalli, JE Griffin, and SG Walker. Slice sampling mixture models. *Statistics and Computing*, 21(1):93–105, September 2011. ISSN 0960-3174. doi:10.1007/s11222-009-9150-y.
- Hugh A Chipman, Edward I George, and Robert E McCulloch. Bayesian CART model search. *Journal of the American Statistical Association*, 93(443):935–948, 1998.
- David GT Denison, Bani K Mallick, and Adrian FM Smith. A Bayesian CART algorithm. *Biometrika*, 85(2):363–377, 1998.
- Jean Diebolt and Christian P Robert. Estimation of finite mixture distributions through Bayesian sampling. *Journal of the Royal Statistical Society. Series B*, pages 363–375, 1994.
- Radford M Neal. Slice sampling. *Annals of Statistics*, pages 705–741, 2003.
- Yeonseung Chung and David Dunson. Nonparametric bayes conditional distribution modeling with variable selection. *Journal of the American Statistical Association*, 2012.
- Yinpu Li, Antonio R. Linero, and Jared S. Murray. Adaptive conditional distribution estimation with Bayesian decision tree ensembles, 2020.
- Sean Plummer, Shuang Zhou, Anirban Bhattacharya, David Dunson, and Debdeep Pati. Statistical guarantees for transformation based models with applications to implicit variational inference. In *The 24th Intl. Conference on Artificial Intelligence and Statistics, AISTATS 2021*, 2021.
- Shen Ghosal, Jayanta K. Ghosh, and A.W. van der Vaart. Convergence Rates of Posterior Distributions. *Annals of Statistics*, 28(2):500–531, 2000.
- Jennifer Starling, Jared Murray, Carlos Carvalho, Radek Bukowski, and James Scott. BART with targeted smoothing: An analysis of patient-specific stillbirth risk. *Annals of Applied Statistics*, 14(1), 2020.
- Alejandro Jara, Timothy Hanson, Fernando A. Quintana, Peter Müller, and Gary L. Rosner. DPpackage: Bayesian Semi- and Nonparametric Modeling in R. *Journal of Statistical Software*, 40(5), 2011.
- Katherine Elizabeth Castellano and Andrew Dean Ho. Contrasting OLS and quantile regression approaches to student “growth” percentiles. *Journal of Educational and Behavioral Statistics*, 38(2):190–215, 2013.
- D Betebenner. Norm-and criterion-referenced student growth. *Educational Measurement: Issues and Practice*, 28(4): 42–51, 2009.
- Damian W Betebenner. A technical overview of the student growth percentile methodology: Student growth percentiles and percentile growth projections/trajectories. the national center for the improvement of educational assessment, 2011.
- Matthew T. Pratola, Hugh A. Chipman, James R. Gattiker, David M. Higdon, Robert McCulloch, and William N. Rust. Parallel Bayesian additive regression trees. *Journal of Computational and Graphical Statistics*, 23(3):830–852, 2014. doi:10.1080/10618600.2013.841584.
- Justin Bleich and Adam Kapelner. Bayesian Additive Regression Trees With Parametric Models of Heteroskedasticity. *arXiv preprint arXiv:1402.5397*, February 2014.
- Shen Ghosal and Aad van der Vaart. Convergence Rates of Posterior Distributions for Noniid Observations. *Annals of Statistics*, 35:192–223, 2007.
- Stan Development Team. RStan: the R interface to Stan, 2020. R package version 2.21.2.

8 Supplement

8.1 BART

In this section, we review the basic details of Bayesian Additive Regression Trees (BART). We refer the reader to Chipman et al. [2010] for a full exposition.

8.1.1 Model and Priors

Chipman et al. consider the regression model

$$y_i = f(\mathbf{x}_i) + \epsilon_i, \epsilon_i \stackrel{iid}{\sim} N(0, \sigma^2)$$

and place a BART prior on f . Such a prior represents the function as the sum of m many piecewise constant regression trees. Each tree T_h , $1 \leq h \leq m$ consists of a set of interior decision nodes (where decisions are generally of the form $x_j < c$ for some value c) and a set of b_h terminal nodes. The terminal nodes have associated parameters $M_h = (\mu_{h1}, \mu_{h2}, \dots, \mu_{hb_h})'$. For each tree there is a partition of the covariate space $\{\mathcal{A}_{h1}, \dots, \mathcal{A}_{hb_h}\}$ with each element of the partition corresponding to a terminal node. A tree and its associated parameters define step functions:

$$g(\mathbf{x}, T_h, M_h) = \mu_{hb} \text{ if } \mathbf{x} \in \mathcal{A}_{hb} \text{ (for } 1 \leq b \leq b_h). \quad (25)$$

These functions are additively combined to obtain f :

$$f(\mathbf{x}) = \sum_{h=1}^m g(\mathbf{x}, T_h, M_h). \quad (26)$$

In the spirit of boosting, each term in the sum is constrained by a strong prior to be a ‘‘weak learner’’; that is, the prior on (T_h, M_h) strongly favors small trees and leaf parameters that are near zero. Each tree independently follows the prior described by Chipman et al. [1998], where the probability that a node at depth d splits (is not terminal) is given by

$$\alpha(1+d)^{-\beta}, \quad \alpha \in (0, 1), \quad \beta \in [0, \infty). \quad (27)$$

A variable to split on, and a cutpoint to split at, are then selected uniformly at random from the available splitting rules. We follow CGM throughout by taking $\alpha = 0.95$ and $\beta = 2$. Traditionally the prior on cutpoints for the j^{th} variable is a discrete uniform distribution over a uniformly spaced grid or some collection of quantiles of $\{x_{ij} : 1 \leq i \leq n\}$. Most implementations of tree-based models also require that the terminal nodes not be empty, or contain at least 5 observations.

To set the priors on M , CGM suggest scaling the data to lie in ± 0.5 and assign the leaf parameters independent priors:

$$\mu_{hb} \sim N(0, \sigma_\mu^2) \quad \text{where } \sigma_\mu = 1/(2k\sqrt{m}). \quad (28)$$

CGM recommend $1 \leq k \leq 3$, with $k = 2$ as a reasonable default choice. This prior shrinks $g_l(x)$ strongly toward zero, while ensuring that the induced prior for $f(x)$ is centered at zero and puts approximately 95% of the prior mass within ± 0.5 . Larger values of k imply increasing degrees of shrinkage. Performance is fairly insensitive to the number of trees m , as long as it is large enough. In practice, $m = 200$ is a common choice.

8.1.2 Posterior Sampling

Chipman et al. [2010] provide full details of the MCMC algorithm used to fit BART. A key ingredient of the sampler is performing blocked updates for $(T_h, M_h \mid \{(T_l, M_l)_{l \neq h}, -\})$. This ‘‘backfitting’’ step utilizes the fact that the full conditional for (T_h, M_h) depends on $\{(T_l, M_l)_{l \neq h}$ and y only through the residuals

$$R_{hi} = \left(y_i - \sum_{l \neq h}^m g(\mathbf{x}_i, T_l, M_l) \right) \sim N(g(\mathbf{x}_i, T_h, M_h), \sigma^2), \quad (29)$$

These residuals follow the single tree model studied by Chipman et al. [1998] with parameters (T_h, M_h, σ^2) , so the Chipman et al. [1998] Metropolis-Hastings update can be embedded within the BART Gibbs sampler to sample (T_h, M_h) jointly from their full conditional. Since M_h has a normal prior, the integrated likelihood $p(R_h \mid T_h, \sigma^2)$ is available in closed form. Therefore (T_h, M_h) can be updated in a block by sampling T_h marginally over M_h with a Metropolis step and then sampling M_h from its full conditional given the new T_h . Complete details including proposal distributions are given in Chipman et al. [1998] (the results in this paper use a smaller set of proposal distributions, outlined in Pratola et al. [2014]). This blocked update enhances mixing and obviates the need for transdimensional MCMC algorithms due to the changing dimensionality of M_h .

8.2 Details on Heteroscedastic Regression with BART priors

8.2.1 Model and Priors

Here, we give an overview of the Murray [2021] extension of the BART prior to model variance functions. Begin with the loglinear model

$$v(x) = \sum_{h=1}^{m_v} g(\mathbf{x}, T_h^{(v)}, M_h^{(v)}) \quad (30)$$

where $\{(T_h^{(v)}, M_h^{(v)})\}$ are trees and parameters for the variance functions. To collect posterior samples, a variant of the backfitting MCMC algorithm is possible. Suppose we are updating $(T_h^{(v)}, M_h^{(v)})$. The first step is constructing the scaled residuals

$$R_{hi}^{(v)} = \frac{(Y_i - f(x_i))}{\exp[\sum_{l \neq h}^m g(\mathbf{x}, T_l^{(v)}, M_l^{(v)})]}. \quad (31)$$

Now $R_{hi}^{(v)} \sim N(0, \sigma^2 \exp[g(\mathbf{x}, T_h^{(v)}, M_h^{(v)})])$ so we have

$$p(R_h^{(v)} | T_h^{(v)}, M_h^{(v)}, \sigma^2) = \prod_{l=1}^{b_h^{(v)}} \prod_{i: \mathbf{x}_i \in \mathcal{A}_l} \frac{1}{\sigma_0 \exp[\mu_{hl}^{(v)}/2]} \phi\left(\frac{R_{ih}^{(v)}}{\sigma_0^2 \exp[\mu_{hl}^{(v)}]}\right) \quad (32)$$

As a normal prior for $\mu_{hb}^{(v)}$ is no longer conditionally conjugate, Murray introduces another prior which is symmetric about 0 on the log scale and also admits closed form representations for the integrated likelihood and full conditional distribution. This prior is specified as an equal probability mixture of gamma and inverse gamma distributions with the same parameters. Let $\tau_{hb}^{(v)} := \exp(\mu_{hb}^{(v)})$. Then, the prior is:

$$p(\tau_{hb}^{(v)}) = \frac{1}{2} \frac{b^a}{\Gamma(a)} (\tau_{hb}^{(v)})^{-a-1} \exp(-b/\tau_{hb}^{(v)}) + \frac{1}{2} \frac{b^a}{\Gamma(a)} (\tau_{hb}^{(v)})^{a-1} \exp(-b\tau_{hb}^{(v)}) \quad (33)$$

Throughout this paper we take $a = b = a_0 m_v$. To motivate this choice, note that if $\tau_{hb}^{(v)}$ has density (33) with $a = b = a_0 m_v$ then $\log(\tau_{hb}^{(v)}) \stackrel{d}{=} (-1)^{Z_h} \log(W_h)$ where $Z_h \stackrel{iid}{\sim} \text{Bern}(0.5)$ and $W_h \stackrel{iid}{\sim} \text{Ga}(a_0 m_v, a_0 m_v)$. The first two moments of $\log(\tau_{hb}^{(v)})$ are 0 and $(a_0 m_v)^{-1}$ and for large $a_0 m_v$ its distribution is nearly normal since the Gamma distributions are so concentrated near 1. Thus, marginally, $v(x)$ will be approximately distributed $N(0, 1/a_0)$ and can be scaled to match the *a priori* expected range of the log-variance process. Even for relatively small $a_0 m_v$ this approximation is excellent; see Figure 12. The marginal prior for $\log(v(x))$ is nearly normal for $a_0 m_v = 5$ and is indistinguishable from the normal density when $a_0 m_v$ is greater than 25. In practice m_v will generally be at least 100. To set a_0 , note that $a_0 = [\log(\sqrt{d})]^{-2}$ implies that $\Pr(\exp[v(\mathbf{x})] \in (\sigma_0^2/d, d\sigma_0^2)) \approx 0.95$. For example, taking $a_0 = 1.5$ makes d about 5. In practice, values of d around 2-4 tend to work well; much larger and the risk of overfitting and degenerate bandwidths increases.

8.2.2 Posterior Sampling

Let $n_{hb} = \sum_{i=1}^n \mathbf{1}(\mathbf{x}_i \in \mathcal{A}_{hb}^{(v)})$, the number of observations in leaf b of $T_h^{(v)}$, and let $r_{hb}^2 = \sum_{i=1}^n [R_{hi}^{(v)}]^2 \mathbf{1}(\mathbf{x}_i \in \mathcal{A}_{hb}^{(v)})$ be the sum of squared residuals in each leaf. Under (33) the full conditional distribution for $\tau_{hb}^{(v)}$ is another mixture distribution:

$$p(\tau_{hb}^{(v)} | R_h^{(v)}, \sigma^2) \propto \frac{\Gamma(n_{hb}/2 + a)}{(b + r_{hb}^2/2)^{n_{hb}/2 + a}} p_{IG}(\tau_{hb}^{(v)}, n_{hb}/2 + a, b + r_{hb}^2/2) \\ + \frac{2K_{(n_{hb}/2 - a)}(\sqrt{2br_{hb}^2})}{(2b/r_{hb}^2)^{(a - n_{hb}/2)/2}} p_{GIG}(a - n_{hb}/2, b, r_{hb}^2/2) \quad (34)$$

where $K_p(x)$ is the modified Bessel function of the second kind, p_{IG} is the pdf of an inverse gamma random variable with rate b , and p_{GIG} is the pdf of a generalized inverse Gaussian random variable:

$$p_{GIG}(\tau; \lambda, \psi, \chi) = \frac{(\psi/\chi)^{(\lambda/2)}}{2K_\lambda(\sqrt{\psi\chi})} \tau^{\lambda-1} \exp\left[-\frac{1}{2}(\psi\tau + \chi/\tau)\right] \quad (35)$$

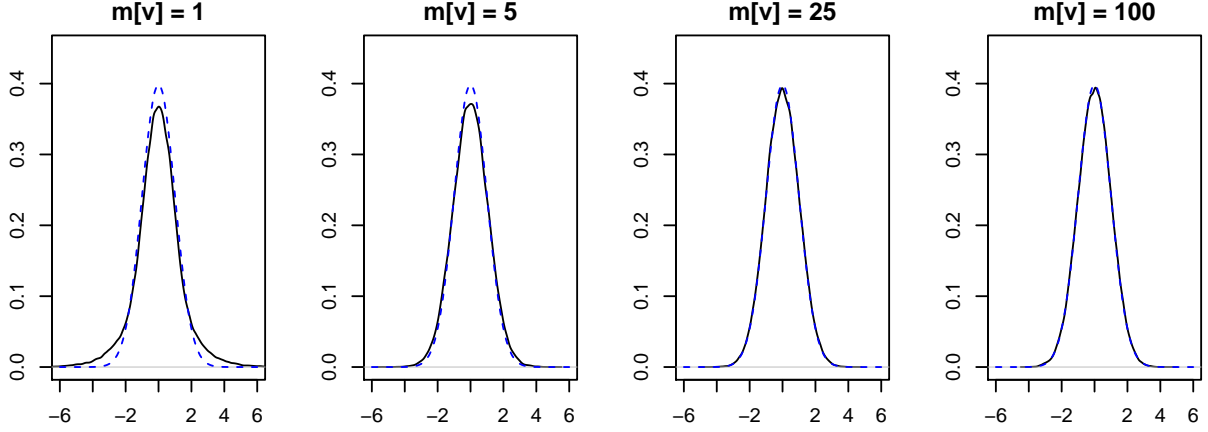


Figure 12: Marginal prior on $v(x)$ for $a_0 = 1$ and a range of m_v . The blue dashed line is the standard normal density.

The integrated likelihood is

$$P(R_h^{(v)} | T_h^{(v)}, \sigma^2) = \prod_{l=1}^{b_h^{(v)}} \frac{1}{2(2\pi)^{n_{hl}/2}} \frac{b^a}{\Gamma(a)} \left(\frac{\Gamma(n_{hl}/2 + a)}{(b + r_{hl}^2/2)^{n_{hl}/2+a}} + \frac{2K_{(n_{hl}/2-a)}(\sqrt{2br_{hl}^2})}{(2b/r_{hl}^2)^{(a-n_{hl}/2)/2}} \right). \quad (36)$$

Block updating $(T_h^{(v)}, M_h^{(v)})$ proceeds by substituting the integrated likelihood (36) into the Metropolis step for $T_h^{(v)}$ and drawing $M_h^{(v)}$ by sampling each $\tau_{hb_h}^{(v)}$ from (36). Given v , updates for the rest of the parameters are straightforward although the integrated likelihood and full conditionals also have to be adjusted in the update for (T_h, M_h) to account for the heteroscedastic residuals. See Bleich and Kapelner [2014] for details.

8.3 Proofs of Theorems

Proof of Theorem 1

Let N_d be the number of nodes at depth d of a tree sampled from this prior. There are 2^{d-1} pairs of possible nodes at depth d . Label these pairs by $1 \leq i \leq 2^{d-1}$ and define $U_i^{(d)}$ as 1 if the i^{th} pair of nodes exists and 0 otherwise, so that $N_d = \sum_{i=1}^{2^{d-1}} 2U_i^{(d)}$. Now $U_i^{(d)} = 1$ if and only if all its parents are splitting nodes, so $\Pr(U_i^{(d)} = 1) = \mathbb{E}(U_i^{(d)}) = \prod_{s=0}^{d-1} \alpha(1+s)^{-\beta} = \alpha^d (d!)^{-\beta}$. Then $E(N_d) = \sum_{i=1}^{2^{d-1}} 2\alpha^d (d!)^{-\beta} = (2\alpha)^d (d!)^{-\beta}$. Since N_d is nonnegative, $\Pr(N_d \geq 1) \leq E(N_d)$. Since $\sum_{d=0}^{\infty} E(N_d) = \sum_{d=0}^{\infty} (2\alpha)^d (d!)^{-\beta} < \infty$, $\Pr(N_d \geq 1 \text{ i.o.}) = 0$ so the tree is almost surely finite.

Proof of Theorem 2

As discussed in Section 4, we must find constants C_1, \dots, C_4 and a sieve \mathcal{G}_n that allow us to verify conditions G1, G2, and G3. We first prove the conditions using Lemmas 1–3; in the next subsection we prove a series of Lemmas allowing us to establish Lemma 3.

Proof of G1. Let $\delta_n = (\log n/n)^{\beta/(2\beta+d_0)}$ and let $\tilde{\epsilon}_n = (\log n/n)^{\frac{\alpha}{\alpha+1} \times \frac{\beta}{2\beta+d_0}}$.

Applying Lemma 3 with $\epsilon = \tilde{\epsilon}_n$, for sufficiently large n we have

$$\begin{aligned} -\log \Pi\{\text{KL}_{p_0}(C_{\text{KL}}\tilde{\epsilon}_n)\} &\leq -\log \Pi(S = S_0) - \log \Pi(\|f - f_0\|_{\infty} \leq \delta_n | S = S_0) \\ &\quad - \log \Pi\{\sigma(\mathbf{x}, u) \equiv \sigma \text{ is constant}, \sigma \in [\tilde{\epsilon}_n^{1/\alpha}, 2\tilde{\epsilon}_n^{1/\alpha}] | S = S_0\}. \end{aligned} \quad (37)$$

As argued by Jeong and Rockova [2020], P1 implies $-\log \Pi(S = S_0) \lesssim d_0 \log(p+1) \lesssim n\epsilon_n^2$. Next, by Lemma 1 we have $-\log \Pi(\|f - f_0\|_{\infty} \leq \delta_n | S = S_0) \lesssim n\delta_n^2 \lesssim n\epsilon_n^2$. Finally, note that with $\sigma_n = \tilde{\epsilon}_n^{1/\alpha}$, by P4 and standard

properties of the inverse gamma distribution we can bound the final term of (37) by

$$\begin{aligned} -\log \Pi\{e^\xi \in [1.2\sigma_n, 1.8\sigma_n], \sup_{hl} |\mu_{hl}^{(v)}| \leq 0.1/m_v, \text{ all trees have depth } 0 \mid S = S_0\} \\ \lesssim -\log \Pi\{e^\xi \in [1.2\sigma_n, 1.8\sigma_n]\} \lesssim \sigma_n^{-1} \lesssim n\epsilon_n^2. \end{aligned}$$

Combining these facts, we get $-\log \Pi\{\text{KL}_{p_0}(C_{\text{KL}}\tilde{\epsilon}_n)\} \lesssim n\epsilon_n^2$, and because $\tilde{\epsilon}_n \leq \epsilon_n$ this implies that G1 holds for some choice of C_1 and C_2 . \square

Proof of G2 and G3. Let κ be a large constant to be determined later and define \mathcal{F}_f as in Lemma 2 with the choices $d = \kappa n\epsilon_n^2 / \log(p+1)$, $K = \lfloor \kappa n\epsilon_n^2 / \log n \rfloor$, $U^2 = \kappa n\epsilon_n^2$, and $\epsilon = \epsilon_n / (n\epsilon_n^2)$. Let \tilde{v} denote the tree-based contribution to the variance function, without the intercept: $\tilde{v} := v(\mathbf{x}, u) - \xi$. Then, we similarly define $\mathcal{F}_{\tilde{v}}$ but with the choice $\epsilon = \epsilon_n^2$ and $U = V$. Lastly, define $\ell = 1/(\kappa n\epsilon_n^2)$ and $u = e^{\kappa n\epsilon_n^2}$. We take the set \mathcal{G} to be given by

$$\mathcal{G} = \{p_{f,\sigma} : f \in \mathcal{F}_f, \tilde{v} \in \mathcal{F}_{\tilde{v}}, \xi \in [\log \ell, \log u]\}.$$

Let \hat{F}_f and $\hat{F}_{\tilde{v}}$ denote $\epsilon_n / (n\epsilon_n^2)$ and ϵ_n^2 nets of \mathcal{F}_f and $\mathcal{F}_{\tilde{v}}$ respectively and let \hat{R} denote an ϵ_n^2 -net of $[\log \ell, \log u]$. Given a $p_{f_1, \sigma_1} \in \mathcal{G}$ we can find $f_2 \in \hat{F}_f$, $\tilde{v}_2 \in \hat{F}_{\tilde{v}}$, and $\xi_2 \in \hat{R}$ such that, by Lemma 3:

$$h(p_{f_1, \sigma_1}, p_{f_2, \sigma_2}) \leq C_h \left\{ \sqrt{2\epsilon_n^2} + e^{m_v V} \frac{\epsilon_n (\kappa n\epsilon_n^2)}{n\epsilon_n^2} \right\} \leq C_\kappa \epsilon_n,$$

for a global constant C_h and a constant C_κ depending only on the constant κ and the prior. Hence

$$\log N(\mathcal{G}, C_\kappa \epsilon_n, h) \leq \log N(\mathcal{F}_f, \epsilon_n / (n\epsilon_n^2), \|\cdot\|_\infty) + \log N(\mathcal{F}_{\tilde{v}}, \epsilon_n^2, \|\cdot\|_\infty) + \log \frac{\log u + \log \ell^{-1}}{\epsilon_n^2}.$$

By Lemma 2, each term is easily verified to be bounded by a constant multiple of $\kappa n\epsilon_n^2$ so that $\log N(\mathcal{G}, C_\kappa \epsilon_n, h) \lesssim \kappa n\epsilon_n^2$.

Next we compute the complementary probability bound. First, by the union bound:

$$\begin{aligned} \Pi(p \notin \mathcal{G}) &\leq \Pi(\xi < \log \ell) + \Pi(\xi > \log u) + \Pi(D > d) \\ &\quad + \Pi(f \notin \mathcal{F}_f \mid D \leq d) + \Pi(\tilde{v} \notin \mathcal{F}_{\tilde{v}} \mid D \leq d). \end{aligned} \tag{38}$$

Using standard properties of the inverse gamma distribution we have

$$\begin{aligned} \log \Pi(\xi < \log \ell) &\lesssim -\ell^{-1} = -\kappa n\epsilon_n^2, \\ \log \Pi(\xi > \log u) &\lesssim -\log u = -\kappa n\epsilon_n^2. \end{aligned}$$

By P1 we also have $\log \Pi(D > d) \lesssim -d \log(p+1) = -\kappa n\epsilon_n^2$. Next, if $D \leq d$ but $f \notin \mathcal{F}_f$ then either (i) $K_m > K$ for some m where K_m is the number of leaf nodes in tree m or (ii) $K_m \leq K$ for all m , but $\sup_{hl} |\mu_{hl}| > U$. Hence, by the tail properties of Gaussian random variables,

$$\begin{aligned} \Pi(f \notin \mathcal{F}_f \mid D \leq d) &\leq \Pi(K_m > K \text{ for some } m) + \Pi(\sup_{hl} |\mu_{hl}| > U \mid K_m \leq K \text{ for all } m) \\ &\leq m\Pi(K_1 > K) + Kme^{-U^2/(2\sigma_\mu^2)}. \end{aligned}$$

As noted in the proof of Theorem 2 of Jeong and Rockova [2020] we have $\log \Pi(K_1 > K) \lesssim -K \log K \lesssim -\kappa n\epsilon_n^2$ while $-U^2/(2\sigma_\mu^2) \lesssim -\kappa n\epsilon_n^2$ by our choice of U . Hence $\log \Pi(f \notin \mathcal{F}_f \mid D \leq d) \lesssim -\kappa n\epsilon_n^2$ as well, provided that n is sufficiently large. Finally, the only way for $\tilde{v} \notin \mathcal{F}_{\tilde{v}}$ to occur when $D \leq d$ is for at least one tree to have more than K leaf nodes, and we have already seen that the log of this probability is bounded by a constant multiple of $-\kappa n\epsilon_n^2$. Putting all of these facts together and bounding each term of (38) by the maximum, we have

$$\Pi(p \notin \mathcal{G}) \leq \exp\{-C_G \kappa n\epsilon_n^2\}$$

for some small constant C_G depending only on the prior. By taking κ larger than $(C_2 + 4)/C_G$ we have $\Pi(p \notin \mathcal{G}) \leq \exp\{-(C_2 + 4)n\epsilon_n^2\}$ and $\log N(\mathcal{G}, \bar{\epsilon}_n, h) \leq C_5 n\bar{\epsilon}_n^2$ for some constant C_5 and $\bar{\epsilon}_n$ a constant multiple of ϵ_n , as desired. \square

Proof of Supporting Lemmas

As before, we use $a \lesssim b$ to mean there is a positive constant C which can be computed from the prior and p_0 , independent of n and p , such that $a \leq Cb$. Unless otherwise stated, the constant is assumed to be universal in the sense that if we write $f(x; \xi) \lesssim g(x)$ then we have $f(x; \xi) \leq Cg(x)$ for all (x, ξ) (unless ξ is part of the prior or a function of p_0).

Throughout this section, $\phi_\sigma * p_0(y | \mathbf{x})$ denotes the convolution $\int \phi_\sigma(y - z)p_0(z | \mathbf{x}) dz$ where $\phi_\sigma(z) = (2\pi\sigma^2)^{-1/2}e^{-z^2/(2\sigma^2)}$. When $\sigma(\mathbf{x}, u)$ is a constant we note that $\phi_\sigma * p_0(y | \mathbf{x}) = p_{f_0, \sigma}$.

Lemma 4. *Suppose p_0 satisfies Condition F. Then for $\sigma < 1$, we have*

$$p_0(y | \mathbf{x}) \lesssim \phi_\sigma * p_0(y | \mathbf{x})$$

Proof. By Condition F, $p_0(y | \mathbf{x})$ is uniformly bounded and bounded away from 0 on $[0, 1]$. First, if $y \notin [0, 1]$ then we have $\phi_\sigma * p_0(y | \mathbf{x}) > 0 = p_0(y | \mathbf{x})$ so that $\phi_\sigma * p_0(y | \mathbf{x}) > Cp_0(y | \mathbf{x})$ for any positive constant C ; hence we can assume without loss of generality that $y \in [0, 1]$. Let $M = \inf_{y, \mathbf{x}} p_0(y | \mathbf{x})$ and write

$$\begin{aligned} \phi_\sigma * p_0(y | \mathbf{x}) &= \int_0^1 \phi_\sigma(y - z)p_0(z | \mathbf{x}) dz \\ &\geq M \int_0^1 \phi_\sigma(y - z) dz \\ &= M \int_{y-1}^y \phi_\sigma(u) du. \\ &\geq M \int_0^1 \phi_\sigma(u) du \geq M/3 \geq \frac{M}{3 \sup_{y, \mathbf{x}} p_0(y | \mathbf{x})} p_0(y | \mathbf{x}), \end{aligned}$$

where the second inequality follows from the fact $U(y; \sigma) = \Phi\{y/\sigma\} - \Phi\{(y-1)/\sigma\}$ is minimized at $y = 1$ for $y \in [0, 1]$ and all σ , and the third inequality follows from the fact that $U(1; \sigma) > 1/3$ for all $\sigma < 1$. Hence $\phi_\sigma * p_0(y | \mathbf{x}) \gtrsim p_0(y | \mathbf{x})$ for $\sigma < 1$. \square

Lemma 5. *If p_0 satisfies Condition F and $\sigma(\mathbf{x}, u)$ is constant with $\sigma < 1$ then*

$$\log \|p_0/p_{f, \sigma}\|_\infty \leq C_{\text{inf}} + \frac{\|f - f_0\|_\infty^2}{\sigma^2},$$

for some C_{inf} .

Proof. The proof is essentially the same as the proof of Lemma 6.2 of Zhou et al. [2017]. We write

$$\begin{aligned} p_{f, \sigma}(y | \mathbf{x}) &= \frac{1}{\sqrt{2\pi}\sigma} \int_0^1 \exp\left\{-\frac{(y - f(\mathbf{x}, u))^2}{2\sigma^2}\right\} \\ &\geq \sqrt{2} \exp\{-\|f - f_0\|_\infty^2/\sigma^2\} \int_0^1 \frac{1}{\sqrt{2\pi}\sigma^2/2} \exp\left\{-\frac{(y - f_0(\mathbf{x}, u))^2}{\sigma^2}\right\} \\ &= \sqrt{2} \exp\{-\|f - f_0\|_\infty^2/\sigma^2\} \phi_{\sigma/\sqrt{2}} * p_0(y | \mathbf{x}). \end{aligned}$$

Therefore, using the fact that $\phi_{\sigma/\sqrt{2}} * p_0(y | \mathbf{x}) \gtrsim p_0(y | \mathbf{x})$ we have

$$\log \frac{p_0(y | \mathbf{x})}{p_{f, \sigma}(y | \mathbf{x})} \leq C_{\text{inf}} + \frac{\|f - f_0\|_\infty^2}{\sigma^2}$$

for some constant C_{inf} . \square

Lemma 6. *Let p_0 satisfy Condition F. Then $\|p_0 - \phi_\sigma * p_0\|_\infty \lesssim \sigma^\alpha$ for sufficiently small σ .*

Proof. Suppose $\alpha \leq 1$. Let $L = \sup_{(y,\mathbf{x}) \neq (y',\mathbf{x}')} \frac{|p_0(y|\mathbf{x}) - p_0(y'|\mathbf{x}')|}{\|(y-y',\mathbf{x}-\mathbf{x}')\|^\alpha}$, which is finite by Condition F. Then:

$$\begin{aligned} |p_0(y|\mathbf{x}) - \phi_\sigma * p_0(y|\mathbf{x})| &= |p_0(y|\mathbf{x}) - \int \phi_\sigma(u) p_0(y-u|\mathbf{x}) du| \\ &= \left| \int p_0(y|\mathbf{x}) \phi_\sigma(u) du - \int \phi_\sigma(u) p_0(y-u|\mathbf{x}) du \right| \\ &\leq \int |p_0(y|\mathbf{x}) \phi_\sigma(u) - p_0(y-u|\mathbf{x}) \phi_\sigma(u)| du \\ &\leq L \int |u|^\alpha \phi_\sigma(u) du \lesssim \sigma^\alpha. \end{aligned}$$

For $1 < \alpha \leq 2$, let $\dot{p}_0(y|\mathbf{x}) = \frac{d}{dy} p_0(y|\mathbf{x})$ and let $L = \sup_{(y,\mathbf{x}) \neq (y',\mathbf{x}')} \frac{|\dot{p}_0(y|\mathbf{x}) - \dot{p}_0(y'|\mathbf{x}')|}{\|(y,\mathbf{x}) - (y',\mathbf{x}')\|^{\alpha-1}}$, which is finite by Condition F.

Then:

$$p_0(y-u|\mathbf{x}) = p_0(y|\mathbf{x}) - u\dot{p}_0(y'|\mathbf{x}) + u\dot{p}_0(y) - u\dot{p}_0(y|\mathbf{x})$$

for some y' between y and $y-u$, depending on (y, \mathbf{x}, u) . Integrating with respect to $\phi_\sigma(u)$, the term $u\dot{p}_0(y|\mathbf{x})$ drops; then taking the absolute value we have:

$$\left| \int (p_0(y-u|\mathbf{x}) - p_0(y|\mathbf{x})) \phi_\sigma(u) du \right| = \left| \int u(\dot{p}_0(y|\mathbf{x}) - \dot{p}_0(y'|\mathbf{x})) \phi_\sigma(u) du \right|$$

The left hand side becomes $|p_0(y|\mathbf{x}) - \phi_\sigma * p_0(y|\mathbf{x})|$ and the right hand side is upper bounded by:

$$\int |u(\dot{p}_0(y) - \dot{p}_0(y')) \phi_\sigma(u)| du \leq L \int |u|^\alpha \phi_\sigma(u) du \lesssim \sigma^\alpha$$

yielding the stated result. \square

Lemma 7. *Suppose Condition F holds. Then for sufficiently small σ we have*

$$\int p_0(y|\mathbf{x}) \log \frac{p_0(y|\mathbf{x})}{\phi_\sigma * p_0(y|\mathbf{x})} dy F_{\mathbf{X}}(d\mathbf{x}) \lesssim \sigma^{2\alpha}.$$

Proof. For fixed \mathbf{x} we can bound the Kullback-Leibler divergence in terms of the chi-squared divergence as

$$\int p_0(y|\mathbf{x}) \log \frac{p_0(y|\mathbf{x})}{\phi_\sigma * p_0(y|\mathbf{x})} dy F_{\mathbf{X}}(d\mathbf{x}) \leq \int \frac{(p_0(y|\mathbf{x}) - \phi_\sigma * p_0(y|\mathbf{x}))^2}{\phi_\sigma * p_0(y|\mathbf{x})} dy F_{\mathbf{X}}(d\mathbf{x}).$$

By Lemma 4 and Condition F, we have that the denominator is bounded away from 0 for small enough σ . Lemma 6 further tells us that the numerator is $O(\sigma^{2\alpha})$, giving the result. \square

Proof of Lemma 3

We first establish the second statement. Let $h_{\mathbf{x}}^2(p, q) = \int \{p(y|\mathbf{x})^{1/2} - q(y|\mathbf{x})^{1/2}\}^2 dy$ denote the usual Hellinger distance between $p(\cdot|\mathbf{x})$ and $q(\cdot|\mathbf{x})$. We begin by noting that, by Cauchy-Schwarz,

$$p_{f_1, \sigma_1}(y|\mathbf{x}) p_{f_2, \sigma_2}(y|\mathbf{x}) \geq \left\{ \int_0^1 \sqrt{\phi_{\sigma_1}(y - f_1(\mathbf{x}, u)) \phi_{\sigma_2}(y - f_2(\mathbf{x}, u))} dy \right\}^2.$$

By Fubini's Theorem and the usual formula for the affinity between normal distributions we have

$$\begin{aligned} h_{\mathbf{x}}^2(p_{f_1, \sigma_1}, p_{f_2, \sigma_2}) &\leq 1 - \int_0^1 \int \sqrt{\phi_{\sigma_1}(y - f_1(\mathbf{x}, u)) \phi_{\sigma_2}(y - f_2(\mathbf{x}, u))} dy du \\ &= \int_0^1 1 - \sqrt{\frac{2\sigma_1(\mathbf{x}, u)\sigma_2(\mathbf{x}, u)}{\sigma_1(\mathbf{x}, u)^2 + \sigma_2(\mathbf{x}, u)^2}} \exp\left\{-\frac{(f_1(\mathbf{x}, u) - f_2(\mathbf{x}, u))^2}{4(\sigma_1(\mathbf{x}, u)^2 + \sigma_2(\mathbf{x}, u)^2)}\right\} du \end{aligned} \quad (39)$$

By the triangle inequality we have $h_{\mathbf{x}}^2(p_{f_1, \sigma_1}, p_{f_2, \sigma_2}) \leq 2\{h_{\mathbf{x}}^2(p_{f_1, \sigma_1}, p_{f_1, \sigma_2}) + h_{\mathbf{x}}^2(p_{f_1, \sigma_2}, p_{f_2, \sigma_2})\}$. Now, note from the inequality $1 - e^{-|x|} \leq |x|$ that for any σ_1, σ_2 we have

$$1 - \sqrt{\frac{2\sigma_1\sigma_2}{\sigma_1^2 + \sigma_2^2}} \leq 1 - \sqrt{\frac{\sigma_1^2 \wedge \sigma_2^2}{\sigma_1^2 \vee \sigma_2^2}} = 1 - \exp\{-|\log \sigma_1 - \log \sigma_2|\} \leq |\log \sigma_1 - \log \sigma_2|.$$

Hence using (39) with f_1 in place of f_2 gives

$$h_{\mathbf{x}}^2(p_{f_1, \sigma_1}, p_{f_1, \sigma_2}) \leq \int_0^1 |\log \sigma_1(\mathbf{x}, u) - \log \sigma_2(\mathbf{x}, u)| du \leq \|\log \sigma_1 - \log \sigma_2\|_{\infty}.$$

Next, we use (39) with σ_2 in place of σ_1 to get

$$\begin{aligned} h_{\mathbf{x}}^2(p_{f_1, \sigma_2}, p_{f_2, \sigma_2}) &\leq \int_0^1 1 - \exp \left\{ -\frac{(f_1(\mathbf{x}, u) - f_2(\mathbf{x}, u))^2}{4\sigma_2(\mathbf{x}, u)^2} \right\} du \\ &\leq \int_0^1 \frac{(f_1(\mathbf{x}, u) - f_2(\mathbf{x}, u))^2}{4\sigma_2(\mathbf{x}, u)^2} du \\ &\leq \frac{\|f_1 - f_2\|_{\infty}^2}{4 \inf_u \sigma_2(\mathbf{x}, u)^2}. \end{aligned}$$

Putting these together we get

$$h_{\mathbf{x}}^2(p_{f_1, \sigma_1}, p_{f_2, \sigma_2}) \leq 2 \left\{ \|\log \sigma_1 - \log \sigma_2\|_{\infty} + \frac{\|f_1 - f_2\|_{\infty}^2}{4 \inf_u \sigma_1(\mathbf{x}, u)^2 \wedge \sigma_2(\mathbf{x}, u)^2} \right\}.$$

Integrating with respect to $F_{\mathbf{X}}(d\mathbf{x})$ and taking the square root gives the result.

To prove the first bound, fix \mathbf{x} and suppose $p_{f, \sigma}$ is such that $\sigma(\mathbf{x}, u)$ is constant, $\sigma \in (\epsilon^{1/\alpha}, 2\epsilon^{1/\alpha})$, and $\|f - f_0\|_{\infty} \leq \epsilon^{1+1/\alpha}$. Note that $\phi_{\sigma} * p_0 = p_{f_0, \sigma}$. For any $p_{f, \sigma}$, applying the triangle inequality we have

$$h_{\mathbf{x}}^2(p_0, p_{f, \sigma}) \leq 2\{h_{\mathbf{x}}^2(p_0, p_{f_0, \sigma}) + h_{\mathbf{x}}^2(p_{f_0, \sigma}, p_{f, \sigma})\}.$$

Using the fact that $h_{\mathbf{x}}^2(p, q) \leq \int p \log(p/q) dy$, the proof of Lemma 7 gives $h_{\mathbf{x}}^2(p_0, p_{f_0, \sigma}) \lesssim \sigma^{2\alpha} \lesssim \epsilon^2$ for sufficiently small ϵ . Next, we have

$$h_{\mathbf{x}}^2(p_{f_0, \sigma}, p_{f, \sigma}) \leq 1 - \exp \left\{ -\frac{\|f - f_0\|_{\infty}^2}{8\sigma^2} \right\} \lesssim \frac{\|f - f_0\|_{\infty}^2}{\sigma^2} \lesssim \frac{\epsilon^{2+2/\alpha}}{\epsilon^{2/\alpha}} \lesssim \epsilon^2.$$

Combining these facts and integrating with respect to $F_{\mathbf{X}}(d\mathbf{x})$ gives $h^2(p_0, p_{f, \sigma}) \lesssim \epsilon^2$. An application of Lemma 8 of Ghosal and van der Vaart [2007] and Lemma 5 gives $K(p_0 \| p_{f, \sigma}) \lesssim \epsilon^2$ and $V(p_0 \| p_{f, \sigma}) \lesssim \epsilon^2$ as well; let C_{KL} denote the constant which makes $\text{KL}(p_0 \| p_{f, \sigma}) \vee V(p_0 \| p_{f, \sigma}) \leq C_{\text{KL}}^2 \epsilon^2$. Hence $p_{f, \sigma} \in \text{KL}(C_{\text{KL}} \epsilon)$, proving the result.

8.4 Simulation Details

8.4.1 Implementation

Code for conducting these simulations can be found at: <https://github.com/vittorioorlandi/DR-BART>.

Implementation details are as below:

- **DR-BART** DR-BART was implemented in R using the Rcpp package.
- **DR-GP** We implemented DR-GP via the rstan package on CRAN for interfacing with Stan [Stan Development Team, 2020]. We followed Kundu and Dunson [2014], used a squared exponential kernel for the Gaussian Process, and introduced covariates appropriately.
- **SBART-DS** The code for SBART-DS was graciously provided by Li et al.
- **PSBPM** This method was run via the implementation on the author's GitHub at: <https://github.com/david-dunson/probit-stick-breaking>. Prior parameters were as suggested in Chung and Dunson [2012].
- **DPMM** The code for DPMM was taken from version 1.17 of the archived CRAN package DPpackage, which can be found here: <https://cran.r-project.org/src/contrib/Archive/DPpackage/>. Prior parameters were left at their defaults.

All methods were run for 25,000 iterations of burn-in, after which 25,000 posterior samples were saved.

8.4.2 Predicted Coverage and Credible Band Width

Here, we provide additional information on 1. the predictive coverage and 2. the credible band width of each method across various simulation settings. To compute the predictive coverage, an additional $n = 1000$ test points were generated for each run of a simulation. The predicted coverage for a run is the proportion of the test points that were contained in the 95% HDR intervals; the reported values are averages across all runs of a simulation. The reported widths are average widths – across runs of a simulation – of 95% posterior credible bands within the 95% HDR region of the true density. That is, we evaluate credible band width in a high density region of the data. The predictive coverage below shows that all methods except for PSBPM consistently have good predictive coverage. The information on credible bands is useful in conjunction with the coverage results in the main text, as it helps show which of the methods that undercover tend to do so because they are unreasonably confident in their estimates (e.g. DR-GP and PSBPM) versus those that simply do not capture the shape of the density well enough (e.g. SBART-DS).

| x | DR-BART | DPMM | SBART-DS | DR-GP | PSBPM |
|-----|---------|------|----------|-------|-------|
| 0.1 | 0.95 | 0.95 | 0.93 | 0.96 | 0.63 |
| 0.5 | 0.95 | 0.95 | 0.96 | 0.96 | 0.75 |
| 0.8 | 0.99 | 0.97 | 0.97 | 0.99 | 0.00 |

Table 5: Mean predictive coverage of 95% predictive intervals, across runs of Simulation 1.

| x | DR-BART | DPMM | SBART-DS | DR-GP | PSBPM |
|-----|---------|------|----------|-------|-------|
| 0.1 | 0.12 | 0.13 | 0.07 | 0.08 | 0.07 |
| 0.5 | 0.26 | 0.20 | 0.17 | 0.10 | 0.12 |
| 0.8 | 0.67 | 0.33 | 0.27 | 0.20 | 0.00 |

Table 6: Mean 95% credible band width within the true 95% HDR region, averaged across runs of Simulation 1.

| x | DR-BART | DPMM | SBART-DS | DR-GP | PSBPM |
|-----|---------|------|----------|-------|-------|
| 0.1 | 0.31 | 0.1 | 0.07 | 0.05 | 0.08 |
| 0.5 | 0.53 | 0.1 | 0.17 | 0.07 | 0.12 |
| 0.8 | 1.55 | 0.3 | 0.27 | 0.20 | 0.00 |

Table 7: Mean 95% credible band width within the true 95% HDR region, averaged across runs of Simulation 2.

8.5 Applications

Code for performing these analyses can be found at: <https://github.com/vittorioorlandi/DR-BART>. The data for the application on returns to education can be found here. The data for the student growth application can be found in the SGPdata R package.

| x | DR-BART | DPMM | SBART-DS | DR-GP | PSBPM |
|-----|---------|------|----------|-------|-------|
| 0.1 | 0.92 | 0.94 | 0.93 | 0.90 | 0.64 |
| 0.5 | 0.94 | 0.97 | 0.95 | 0.97 | 0.73 |
| 0.8 | 1.00 | 0.99 | 0.97 | 1.00 | 0.00 |

Table 8: Mean predictive coverage of 95% predictive intervals, across runs of Simulation 2.

| x | DR-BART | DPMM | SBART-DS | DR-GP | PSBPM |
|-----|---------|------|----------|-------|-------|
| 0.1 | 0.95 | 0.95 | 0.94 | 0.96 | 0.61 |
| 0.5 | 0.95 | 0.97 | 0.96 | 0.97 | 0.78 |
| 0.8 | 1.00 | 0.96 | 0.97 | 0.99 | 0.00 |

Table 9: Mean predictive coverage of 95% predictive intervals, across runs of Simulation 3.

| x | DR-BART | DPMM | SBART-DS | DR-GP | PSBPM |
|-----|---------|------|----------|-------|-------|
| 0.1 | 0.11 | 0.13 | 0.07 | 0.08 | 0.07 |
| 0.5 | 0.33 | 0.34 | 0.24 | 0.16 | 0.17 |
| 0.8 | 0.63 | 0.33 | 0.25 | 0.20 | 0.00 |

Table 10: Mean 95% credible band width within the true 95% HDR region, averaged across runs of Simulation 3.